

## Thermal Infrared Imager TIR on Hayabusa2 and Its In-Flight Performance using Earth-Moon Thermal Images.

\*Tatsuaki Okada<sup>1,9</sup>, Tetsuya Fukuhara<sup>2</sup>, Satoshi Tanaka<sup>1,9</sup>, Makoto Taguchi<sup>3</sup>, Takeshi Imamura<sup>1,9</sup>, Takehiko Arai<sup>8</sup>, Hiroki Senshu<sup>4</sup>, Yoshiko Ogawa<sup>5</sup>, Hirohide Demura<sup>5</sup>, Kohei Kitazato<sup>5</sup>, Ryosuke Nakamura<sup>6</sup>, Toru Kouyama<sup>6</sup>, Tomohiko Sekiguchi<sup>7</sup>, Sunao Hasegawa<sup>1</sup>, Tsuneo Matsunaga<sup>8</sup>, Takehiko Wada<sup>1</sup>, Jun Takita<sup>9</sup>, Naoya Sakatani<sup>1</sup>, Yamato Horikawa<sup>10</sup>, Ken Endo<sup>5</sup>, Joern Helbert<sup>11</sup>, Thomas G. Mueller<sup>12</sup>, Axel Hagermann<sup>13</sup>

1.Institute of Space and Astronautical Science, Japan Aerospace Exploration Agency, 2.National Institute of Information and Communications Technology, 3.Rikkyo University, 4.Chiba Institute of Technology, 5.University of Aizu, 6.National Institute of Advanced Industrial Science and Technology, 7.Hokkaido University of Education, 8.National Institute of Environmental Studies, 9.University of Tokyo, 10.Graduate University for Advanced Studies, 11.German Aerospace Center, 12.Max-Planck Institute for Extraterrestrial Physics, 13.Open University

Thermal infrared imager TIR is a remote instrument on Hayabusa2 sample return mission from C-type near-Earth asteroid 162173 Ryugu, organized by Japan Aerospace Exploration Agency (JAXA) [1]. The instrument is based on the uncooled micro-bolometer array inherited from the Longwave Infrared Camera LIR on Akatsuki Venus Orbiter [2]. TIR is to observe thermal emission off the asteroid surface, and investigate its thermo-physical properties. We report here the results of in-flight performance of TIR, especially for observations of Earth and Moon.

TIR consists of the sensor unit (TIR-S) and the power supply unit (TIR-AE), along with the digital electronics (DE) for image data processing and the interface for telemetry and command. A couple of images are taken with its shutter open and close so that an effective thermal image is consequently derived by subtraction of these two images [3].

TIR covers its wide temperature from 150 to 460 K, meaning all the sunlit areas of Ryugu, and even the shadowed areas if the thermal inertia of the surface is higher than 50 [ $\text{tiu} = \text{J m}^{-2} \text{s}^{-0.5} \text{K}^{-1}$ ]. Field of view of TIR is  $16.7^\circ \times 12.7^\circ$  in horizontal and vertical directions with  $328 \times 248$  effective pixels, with IFOV of  $0.051^\circ$  per pixel. This corresponds to about 17 m per pixel from the Home Position, 20 km altitude from asteroid surface. The closest view by TIR is about 1cm from the 10 m altitude during the final approach to touchdown [3].

Performance of TIR has been checked almost monthly. We controlled its temperatures by adjusting the setting points of Heater Control Electronics HCE of Hayabusa2 to investigate temperature dependency of TIR images. TIR observed the deep sky during the checks. TIR images have peripheral brightening due to thermal emission from the hood and optics of TIR. We found the lower detection temperature limit of TIR is about 150K. The effect of peripheral brightening is thoroughly reduced from TIR images by subtracting a deep sky image taken at the same temperature settings. TIR was mounted on the +Y panel of Hayabusa2 spacecraft and pointed to -Z axis. The -Z axis alignment of TIR was surveyed using the images of Earth and Moon taken before and after the Earth swing-by. Alignment of TIR in -Z axis is checked relative to that of spacecraft, and proven within 1 or 2 pixels ( $0.05^\circ$  or  $0.10^\circ$ ) shifted in horizontal and vertical directions [4]. It was the unique opportunity for TIR to observe the Earth and Moon, which are the only targets with known thermo-physical properties in space before arrival at Ryugu. TIR images were taken a few minutes before the Optical Navigation Camera (ONC-T) to compare TIR and ONC-T images. In the Earth's images, Australian Continent is hotter than the surrounding ocean by 10 to 20 °C, the Antarctica is cold at around -45 to -40 °C, the southern Indian Ocean is about 0 °C. Clouds are about -45 to -30 °C. The Moon was imaged only 5 pixels in diameter, but the highest temperature can be estimated as 60 to 70 °C for the area at

medium latitude. This is consistent with the estimated value for the area. The observations of Earth and Moon by TIR show that the surface temperatures are consistent with the estimated values. Thus we believe that thermal images by TIR are expected to make an essential contribution as planned for the exploration of asteroid Ryugu.

Acknowledgments: This research is partly supported by the Grant-in-Aid for Scientific Research (B), No. 26287108, of the Japan Society for the Promotion of Science.

References: [1] Tsuda Y. et al. (2013) *Acta. Astronautica*, 91, 356-362. [2] Fukuhara T. et al. (2011) *Earth Planets Space*, 63, 1009-1018. [3] Okada T. et al. (2016) *submitted to Space Sci. Review*. [4] Arai T. et al. (2016) *Lunar Planetary Sci. Conf.*, submitted.

Keywords: Hayabusa2, asteroid exploration, thermograph, Thermal Infrared Imager, Earth Swing-by, thermal inertia

## Image and database browser for TIR on Hayabusa2

\*Ken Endo<sup>1</sup>, Naru Hirata<sup>1</sup>, Wataru Ueno<sup>1</sup>, Hirohide Demura<sup>1</sup>, Takehiko Arai<sup>2</sup>, Tatsuaki Okada<sup>3</sup>, Satoshi Tanaka<sup>4</sup>

1.The University of Aizu, 2.National Institute for Environmental Studies, 3.Institute of Space and Astronautical Science, Japan Aerospace Exploration Agency, 4.Department of Solid Planetary Sciences Institute of Space and Astronautical Science

1  
Introduction: Hayabusa2 was launched to an asteroid, Ryugu. The spacecraft will arrive at the asteroid in 2018 [1]. Hayabusa2 TIR (Thermal Infrared Imager) [2] science team should complete preparations of analysis. The preparations include development of TIR image viewer and establishment of TIR calibration procedures. Those should be ready until the rendezvous for analyzing observation data. This study is categorized into fields of computer graphics and big data analysis in computer science. This study develop image and database browser. This study has developed two sub systems. One is thermal image viewer. Another is thermal image database for calibration. Thermal calibrations exist 2 ways that using calibration curve and using interpolation based on near parameters by calibration database. Although thermal image viewer exists such as ParaView [3], those viewers don't have calibration system. The former way uses calibration formula such as Arai (2015) [4]. The way converts easily digital number to temperature. On the other hands, lacking precision of the way depends on a calibration formula, because the way based on an approximation. The latter way uses same method such as big data analysis. The way finds matching data or near parameters data from a large amount of data. The way needs a database function. That is thought able to calibrate precisely, but the way requires high calculation costs. The way is a key to develop new type of viewer. Therefore, this study has development of a system of involving viewer and a database for calibration. The system is developed from scratch. Goal of this study is development of software that visualizing TIR exploration data and getting TIR ground test data for calibration. TIR data consists of TIR image and ancillary data. The ancillary data has target information, optical information and environment information.

2  
Requirements: Required functions were decided based on hearing with Hayabusa2 TIR science team. The requirements were divided into 4 items.

- Loading TIR data
- Displaying TIR image and 3D model
- Getting TIR data for a calibration
- Database for ground test of TIR

3  
Development Environments: The environments can develop by open source.

4  
System Design: The system has 6 modules. Those modules are built into 4 components.

- Components
- User Interface
  - Processing
  - Database
  - Converting

- Modules
- Loading TIR data

- Displaying TIR image
- Converting
- Database browser
- Displaying Visualization Toolkit file
- Display 3D model.

5

Calibration database: Calibration database stores TIR data. The database consists thermal image table and pixel information table. This data is obtained by ground test of TIR in JAXA. This study refers to Kuwano (2016) about pixel information table [5].

6

Results: This study considered Trade-off and User feedback.

7

Demonstration: We have a demonstration of this system in this presentation.

8

Discussion: It is developed in this study that the system suitable for analyze. The system should be improved on.

9

Conclusions: This study has developed the system. The system displays TIR image and ancillary data. This system satisfies all requirements.

10

References:

[1] JAXA, website

[http://www.jaxa.jp/press/2015/12/20151214\\_hayabusa2\\_j.html](http://www.jaxa.jp/press/2015/12/20151214_hayabusa2_j.html) (In Japanese)

[2] T. Okada, et al., THERMAL-INFRARED IMAGER TIR ON HAYABUSA2 FOR OBSERVATION OF ASTEROID (162173) 1999JU3.46th Lunar and Planetary Science Conference, 2015.

[3] ParaView, website <http://www.paraview.org>

[4] T. Arai, et al., Thermal Imaging performance of TIR onboard Hayabuse2 Spacecraft, 2015.

[5] S. Kuwano. Image database with query by individual pixel attribute for Hayabusa2 TIR archive, Master's thesis, University of AIZU, Feb 2016.

Keywords: Hayabuse2, Database, TIR

## Curation works for the Hayabusa samples and development for Hayabusa2 sample curation facility

\*Toru Yada<sup>1</sup>, Masanao Abe<sup>1</sup>, Tatsuaki Okada<sup>1</sup>, Hisayoshi Yurimoto<sup>3</sup>, Masayuki Uesugi<sup>1</sup>, Yuzuru Karouji<sup>1</sup>, Aiko Nakato<sup>1</sup>, Minako Hashiguchi<sup>1</sup>, Toru Matsumoto<sup>1</sup>, Masahiro Nishimura<sup>2</sup>, Kazuya Kumagai<sup>1</sup>, Shigeo Matsui<sup>1</sup>, Masaki Fujimoto<sup>1</sup>

1.Japan Aerospace Exploration Agency, 2.Marine Works Japan, 3.Hokkaido University

Hayabusa spacecraft successfully returned its reentry capsule including regolith samples of S-type asteroid Itokawa to the Earth in 2010 [1, 2]. Their preliminary examinations revealed that they are similar to equilibrated LL chondrite [3]. JAXA astromaterial sample research group (ASRG) conducted international announcement of opportunity (AO) for Hayabusa-returned samples twice from FY2012 to FY2013. With the two AOs, 32 research proposals have been selected for sample allocations and 112 particles have been distributed to them [4]. Based on results of their researches, it is figured out that space weathering rims on regolith particles are less developed in those from the first touchdown place than the second one [5] and the gas retention age of three Itokawa particles was determined as 1.3 billion years by <sup>40</sup>Ar-<sup>39</sup>Ar dating, which is considered to reflect the age just before or during the catastrophic impact event on the precursor body of the present asteroid Itokawa [6]. The ASRG conducted the 3rd international AO for Hayabusa-returned samples in FY2015. 12 research proposals were selected for sample allocation in Jun 2015, 44 particles for 11 proposals have been distributed until Jan 2016 as we started their distributions in Aug 2015. We are now planning to start international AO in which we will always accept research plan in FY2016. Simultaneously, the ASRG has developed a specification of curation facility for returned samples by Hayabusa2, which was launched in Dec 2014, under the supervision of the specification developing committee for Hayabusa2 sample curation facility [7]. Hayabusa2 will reach C-type asteroid Ryugu in 2018, execute remote-sensing observation, impact crating experiment, and three-times sample collections in a year and half operation there, and return the collected samples to the Earth in Dec 2020. In the committee, we are discussing performances and functions of instruments and facilities in order to start their functional checks and rehearsals for returned sample acceptance in FY2018. We are now considering to equip a function to recover and preserve a certain amount of samples from the sample catcher in vacuum condition. We consider that we will start construction of facilities for Hayabusa2 as early as FY2016.

References: [1] Abe M. et al. (2011) *LPSC XXXXII*, #1638, [2] Yada T. et al. (2014) *Meteoritics Planet. Sci.* 49, 135, [3] Nakamura T. et al. (2011) *Science* 333, 1113. [4] Yada T. et al. (2014) *LPSC XXXXV*, #1759, [5] Noguchi T. et al. (2014) *Earth Planets Space* 66, 124, [6] Park J. et al. (2015) *Meteoritics Planet. Sci.* 50, 2087, [7] Uesugi M. et al. (2015), *Hayabusa 2015 symposium*, [8] Tsuda Y. et al. (2013) *Acta Astronautica* 91, 356.

Keywords: Hayabusa2, Sample return mission, curation, Itokawa, Ryugu, Hayabusa

## Current Status of Hayabusa2 Landing Site Deliberation

\*Aiko Nakato<sup>1</sup>, Hikaru Yabuta<sup>2</sup>, Mutsumi Komatsu<sup>3</sup>, Tomokatsu Morota<sup>4</sup>, Moe Matsuoka<sup>5</sup>, Seiji Sugita<sup>6</sup>, Takaaki Hiroi<sup>7</sup>, Kohei Kitazato<sup>8</sup>, Tatsuaki Okada<sup>1</sup>, Hiroki Senshu<sup>9</sup>, Sho Sasaki<sup>2</sup>, Tomoki Nakamura<sup>4</sup>, Naoki Kobayashi<sup>1</sup>, Seiichiro Watanabe<sup>5</sup>, Hayabusa2 Landing Site Working Group

1.Institute of Space and Astronautical Science, Japan Aerospace Exploration Agency, 2.Osaka University, 3.The Graduate University for Advanced Studies [SOKENDAI], 4.Nagoya University, 5.Tohoku University, 6.The University of Tokyo, 7.Brown University, 8.University of Aizu, 9.Chiba Institute of Technology

Hayabusa2 is scheduled to arrive at the C-type asteroid 162173 Ryugu on July 2018. During its 18-month stay, Hayabusa2 will sample surface materials at three different locations on the asteroid (Yoshikawa et al., 2014). To maximize the scientific gains of Hayabusa2 mission, it is important to select the landing sites from scientific aspects that are derived from integration of remote sensing data obtained by on-board instruments, ONC, NIRS3, TIR, LIDAR, and MASCOT, and laboratory experiment data obtained by using meteorites and simulant of asteroidal materials. Therefore, the Interdisciplinary Science Team which draws the general picture of a scientific scenario of Hayabusa2 (Kobayashi et al., 2014) newly organized four working groups in 2014. The main purpose of these WGs is to select the best landing site by integrating remote sensing data and meteoritical knowledge, and is to expand planetary science into new research fields via the WG process.

Meteorite WG: The primary purpose of this WG is to identify the surface of Ryugu with one of the meteorite groups. Previous studies show that many carbonaceous chondrites are petrologically heterogeneous in a mm-cm scale. Meter-scale observation of the entire surface obtained by Hayabusa2 would contribute to understand the formation history of C-type asteroids including asteroid Ryugu. In order to constrain the meteorite group using the remote sensing data, petrologic variations observed in different meteorite groups and those within a group are being discussed. Brecciation, secondary alteration, and space weathering effects on the asteroid surface are also considered in collaboration with the other WGs.

Secondary alteration WG: We have proposed the following 3 candidates as scientifically valuable samples on Ryugu; (1) major components, (2) primitive materials (here after, 'primitive materials' are supposed to be materials that were experienced the least secondary alteration on the asteroid), and (3) others (e.g. exotic material). Firstly, we discussed the detailed spectral characteristics for identification of the primitive materials on the asteroidal surface using data acquired by the on-board instruments. Reflectance spectra of the primitive materials should show low albedo, no/weak 0.7 and 1  $\mu\text{m}$  absorptions suggesting presence of hydrous minerals and anhydrous silicate respectively, and a clear absorption-band at 3  $\mu\text{m}$  caused by presence of hydrous phases. However, the spectral features of asteroids are complex since they depend on several parameters. Further accumulation of reflectance spectra for various groups of meteorites will be required. The other candidates will be examined as well.

Volatiles WG: Searching organic compounds from the asteroid surface is one of the significant goals of Hayabusa2. In particular, organic carbon contents could be an indicator for a primitive asteroid. For example, the contents of insoluble organic matter (IOM) and total organic carbon (TOC) from CM, CR, and Tagish Lake chondrites negatively correlate with the albedo features at the wavelength of 0.55 and 0.39  $\mu\text{m}$  in their reflectance spectra (Hiroi et al., 2016), respectively. These correlations appear to be related to the aqueous alteration degrees. TOC values are superficially higher in the aqueously altered chondrites. To be more accurate, we propose that the albedos are the better indicator reflecting the ratio of IOM to soluble organic matter (SOM).

Further laboratory experiments must be carried out in order to evaluate the degrees of thermal metamorphism and space weathering.

Grain size WG: The possible methods for determination of the asteroidal surface condition have been organized so far. We continue discussion about the surface condition determination by integrating data from several on-board instruments. In addition, the influence of grain sizes on spectral feature will be evaluated.

Keywords: Hayabusa2, Interdisciplinary Science Team, landing site

Earth-moon images captured by Hayabusa2 visible cameras during Earth swing-by

\*Seiji Sugita<sup>1</sup>, Manabu Yamada<sup>2</sup>, Hiroataka Sawada<sup>3</sup>, Tomokatsu Morota<sup>4</sup>, Rie Honda<sup>5</sup>, Shingo Kameda<sup>6</sup>, Chikatoshi Honda<sup>7</sup>, Hidehiko Suzuki<sup>8</sup>, Toru Kouyama<sup>9</sup>, Kazunori Ogawa<sup>10</sup>, MASATERU ISHIGURO<sup>11</sup>

1.the University of Tokyo, 2.Chiba Institute of Technology, 3.JAXA, 4.Nagoya University, 5.Kochi University, 6.Rikkyo University, 7.Aizu University, 8.Meiji University, 9.AIST, 10.Kobe University, 11.Seoul National University

JAXA's Hayabusa2 completed an Earth swing-by on December 3th of 2015. During this opportunity, we photographed both Earth and Moon with three optical navigation cameras (ONC-T, W1 and W2). Since this was the last opportunity to observe extended light source before reaching the target asteroid Ryugu, the obtained images are extremely important for calibration of our cameras. In this paper, we present the Earth-Moon images and preliminary analysis results.



## The Effect of Rotation Period on Slope Distribution on Asteroid Itokawa

\*Masanori Kanamaru<sup>1</sup>, Sho Sasaki<sup>1</sup>

1.Osaka University

Asteroids 25143 Itokawa was visited by the spacecraft Hayabusa and its detailed surface was unveiled. Demura et al. (2006) reported that Itokawa surface is divided into rough highlands and smooth low lands. Rough areas are covered with lots of boulders. Meanwhile, there are few boulders in smooth areas. It might be the result of regolith migration by seismic shaking (Miyamoto et al. (2007))

Itokawa has very steep slope areas especially on the neck region. "Slope" is defined as the separation angle of a gravity acceleration vector and a normal vector of a surface facet. Non-spherical body like Itokawa has an asymmetric gravity field. Polyhedron model, which was studied in Werner and Scheeres (1997), is an effective way to calculate such an asymmetric gravity field of a polyhedron with homogeneous density. We calculated the surface gravity field and slope distributions, giving Itokawa shape models, observed rotation period (12.1324 hour) and the bulk density (1.95 grams per cubed centimeters). We found that there are many steep slope areas over 30 degrees in the neck region of Itokawa. Such a steep slope looks like unstable.

Change of rotation period is known as YORP effect by solar radiation. As a rotation period changes, a surface gravity field and a slope distribution also change. This phenomenon makes a strong effect on Itokawa's history of reconfiguration and surface terrain formation in hundreds of thousand years time span. This time, we calculated the slope distribution with different rotation period (4h, 6.5h, 9h, 12.1324h, 18h, 24h). It showed that faster rotation can change surface gravity and reduce slope.

One of possible scenarios for Itokawa formation is that Itokawa rotated much faster before and surface topography was formed then. After that, the spin rate may have been decelerated by YORP effect.

S. C. Lowry et al. (2014) studied that observed light curves of Itokawa and simulation of YORP effect and inferred interior density distribution. We expect to simulate the surface gravity with heterogeneous density and make a restriction on internal structure of Itokawa.

Keywords: Asteroid 25143 Itokawa, Gravity field, Slope, YORP effect

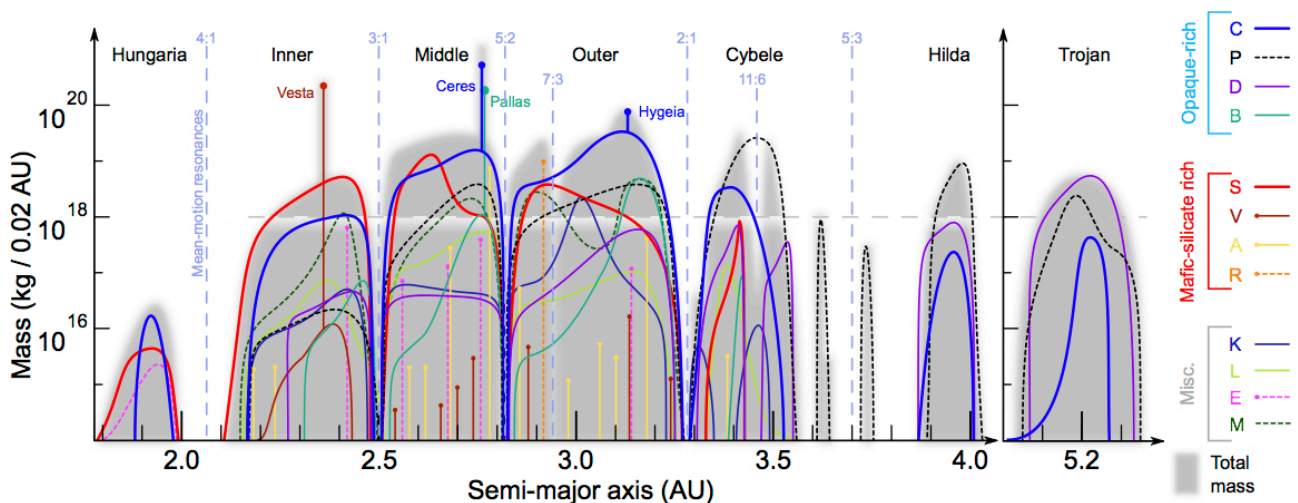
## Asteroids as Records of Solar System History

\*Francesca Eleanora DeMeo<sup>1</sup>, Benoit Carry<sup>2</sup>, David Polishook<sup>3</sup>, Brian Burt<sup>1</sup>, Richard Binzel<sup>1</sup>, Nicholas Moskovitz<sup>4</sup>

1.Massachusetts Institute of Technology, 2.Observatoire de la Cote d'Azur, 3.The Weizmann Institute, 4.Lowell Observatory

Asteroids and other small bodies are markers, like tiny beacons, relaying information about the initial temperature and composition conditions of our Solar System revealed by their surface compositions. The Solar System's evolution may also be determined from the scattering record of these bodies. Today we are armed with major advancements from the past decade that have revolutionized the field of asteroids in areas such as discovery, physical characterization, meteorite links, and dynamical models. Based on tens of thousands of measurements from the Sloan Digital Sky Survey, in this talk I present a new compositional map of the asteroid belt that reveals a greater diversity of asteroids as a function of size and distance and discuss these results in the context of Solar System formation and evolution.

Keywords: asteroid, composition, solar sytem



Fluid flow in hydrous asteroids induced by H<sub>2</sub> gas pressure\*Wataru Fujiya<sup>1</sup>

1. Ibaraki University, College of Science

Physicochemical models on thermal history associated with material evolution of hydrous asteroids have been explored by many authors (e.g., Grimm and McSween 1989; Cohen and Coker 2000). A few models included fluid flow in these bodies to reproduce the characteristic oxygen isotopic compositions of aqueously altered meteorites like CM and CI chondrites (e.g., Young 2001; Palguta et al. 2010). These fluid flow models predicted convective or exhalation flow induced by temperature gradient or vapor pressure. Although these models involved hydration reactions, gas phases such as H<sub>2</sub> produced by the reactions were not taken into account.

Here I present a model on fluid flow in hydrous asteroids considering H<sub>2</sub> gas generated by oxidation of metallic iron. Since H<sub>2</sub> gas pressure in hydrous asteroids is inferred to be hundreds of bars from the amount of metallic iron in primitive chondrites, steep pressure gradient occurs between the surface and interior of the asteroids. The model is 1D spherically symmetric and includes thermal conduction of heat generated by <sup>26</sup>Al decay, phase transition of water/ice, a simplified aqueous alteration reaction, and fluid flow. I assume that the asteroids accreted 2.7 Myr after CAI formation, resulting in the initial <sup>26</sup>Al/<sup>27</sup>Al ratio of 3.7 × 10<sup>-6</sup>. The velocity of fluid flow is derived from the Darcy's law. The radii of the asteroids range from 30-100 km. The initial temperature is 173 K, and the surface temperature is fixed to this value. The asteroids initially consist of 70 vol% rock, 5 % water/ice, and 25 % void space. When liquid water is present, the rock reacts with water and 90 % of the consumed water is assumed to convert to H<sub>2</sub> gas until metallic iron is completely oxidized.

The results of the simulation suggest that fluid (H<sub>2</sub> gas and liquid water) flows outward soon after ice melts and water reacts with rock. However, water stops flowing ~8 km below the surface because temperatures there are lower than the freezing point of water. Then an icy shell forms near the surface, and liquid water accumulates just below the icy shell. As a result, water heterogeneously distributes throughout the asteroids in spite of its initially homogeneous distribution. Water consumed by the alteration reaction amounts to ~1.7-3.1 vol% around the center of the asteroids and to 5.5-16 % below the icy shell, depending on the asteroid sizes. The peak temperatures range from ~800 K around the center to ~370 K in heavily altered regions. These combinations between peak temperatures and alteration degrees are consistent with those inferred for CO and CM chondrites. This may imply that CO and CM chondrites originated from the same parent body, suggested from their oxygen isotopic compositions forming a single regression line in an oxygen three-isotope plot.

Keywords: fluid flow, hydrous asteroids, hydrogen gas

## Experimental study on compression property of granular material

\*Tomomi Omura<sup>1</sup>, Akiko Nakamura<sup>1</sup>

1. Graduate School of Science, Kobe University

Porosity structure inside a planetary body and of surface regolith plays important role in collisional and thermal evolution of the body. The porosity structure is changed by presence of rocks, seismic shaking, thermal evolution, and self-gravity in particular. Porosity structure caused by soil pressure due to self-gravity gives an initial, most-possible porous structure of the body consisting of granular material. Therefore, understanding compression property of granular material is necessary. Compression properties of granular material should be controlled by various parameters such as initial porosity of granular bed, composition, size distribution, and shape of constituent particles. Moreover, the surface energy of constituent particles thought to become 100 times larger in vacuum than in atmosphere (Kimura et al. 2015). The interparticle force, and consequently the compression properties, depends on the surface energy. Therefore, general formula for the compression property of granular material in various environments is required to estimate the porosity structure of planetary bodies.

An empirical formula to estimate the initial porosity of granular bed consisting of monodisperse particles deposited by gravity was introduced by Kiuchi and Nakamura (2014) based on the ratio of interparticle force and gravity. However, this formula is only applicable to the uppermost layer of granular bed because the granular bed at some depth is compressed by soil pressure. During the compaction process of granular bed, the porosity of granular bed is decreased by rearrangements of constituent particles and this rearrangement mechanism changes with coordination number of constituent particle. When the coordination number is less than 6, the constituent particles are rearranged by rolling. When the coordination number exceeds 6, they are rearranged by sliding. The coordination number increases as the porosity decreases. The coordination number reaches 6 when porosity is  $\sim 0.7$  (Wada et al., 2011).

We conducted compression experiments of various kinds of samples. Each sample has different composition and size distribution. Main compositions of the samples are  $\text{Al}_2\text{O}_3$  and  $\text{SiO}_2$  and the particle size is smaller than  $100 \mu\text{m}$ . We sieved these samples into cylindrical container and the top part of the bed over the height of the container was leveled off. Then we compressed the sample by compressive testing machine. The applied pressure was ranged from  $10^4$  to  $2 \times 10^6$  Pa.

The initial porosity of the granular bed was different for different samples and it was in the range of 0.54-0.86. We compared this result with the formula introduced in Kiuchi and Nakamura (2014). We found that this formula can estimate approximate porosity of granular bed constituted by polydisperse particles if we adopt the median diameter of the particles as representative particle diameter. It was shown that the slope of compression curve becomes shallower as the frictional force between particles increases in the range of the pressure between  $10^4$  and  $2 \times 10^6$ . In this range, porosities of samples are less than  $\sim 0.7$ . Size distribution width of sample affects compression properties too and the samples with wider size distribution are compressed easier (Omura et al., ISTS, 2015).

We conducted new compression experiments. We expanded the pressure range to lower than  $10^2$  Pa and we found that compaction process of granular bed is divided into three regimes: (1) Pressure is lower than the strength of granular bed accordingly the granular bed isn't compacted. (2) Granular bed is compacted but the decrease in porosity is gradual. (3) The porosity decline-rate becomes larger than the regime 2. We will further investigate how these boundaries are determined and will present the results.

Keywords: Small body, Porosity, Internal structure, Granular material

## Thermal Modeling of Comet-Like Asteroids

\*Yoonsoo Bach Park<sup>1,2</sup>, MASATERU ISHIGURO<sup>1</sup>, Fumihiko Usui<sup>3</sup>

1.Seoul National University, 2.Korea Advanced Institute of Science and Technology, 3.The University of Tokyo

Recent analysis on asteroidal thermophysical property revealed that there is a tendency that their thermal inertia decrease with their sizes at least for main belt asteroids. However, little is known about the thermal properties of comet-like bodies. In this work we utilized a simple thermophysical model to calculate the thermal inertia of a bare nucleus of comet P/2006 HR30 (Siding Spring) and an asteroid in comet-like orbit 4015 Wilson-Harrington from AKARI observation data. It is also shown that the determination of their thermal inertia is very sensitive to their spin vector, while the diameter is rather easy to be constrained to a certain range by combining multi-wavelength observational data. Thus, we set diameter and hence the geometric albedo as fixed parameters, and inferred the spin vector and thermal inertia of the targets. Further detailed analyses on these cometary bodies will shed light on our understanding of the detailed surfacial characteristics of them.

Keywords: Thermal model, Asteroids, Thermophysical model

## MONITORING OBSERVATIONS OF THE JUPITER-FAMILY COMET 17P/HOLMES DURING ITS 2014 PERIHELION PASSAGE

\*Yuna Grace Kwon<sup>1</sup>, MASATERU ISHIGURO<sup>1</sup>, Hidekazu Hanayama<sup>2</sup>, Daisuke Kuroda<sup>3</sup>, Satoshi Honda<sup>4</sup>, Jun Takahashi<sup>4</sup>, Yoonyoung Kim<sup>1</sup>, Myung Gyoon Lee<sup>1</sup>, Young-Jun Choi<sup>5</sup>, Myung-Jin Kim<sup>5</sup>, Jeremie Vaubailon<sup>6</sup>, Takeshi Miyaji<sup>2</sup>, Kenshi Yanagisawa<sup>3</sup>, Michitoshi Yoshida<sup>7</sup>, Kouji Ohta<sup>8</sup>, Nobuyuki Kawai<sup>9</sup>, Hideo Fukushima<sup>10</sup>, Jun-ichi Watanabe<sup>10</sup>

1.Seoul National University, 2.Ishigakijima Astronomical Observatory, 3.Okayama Astrophysical Observatory, 4.Nishi-Harima Astronomical Observatory, 5.Korea Astronomy and Space Science Institute, 6.Observatoire de Paris, 7.Hiroshima University, 8.Kyoto University, 9.Tokyo Institute of Technology Meguro, 10.National Astronomical Observatory of Japan

Comets are the most pristine reservoir of the materials left over from the formation epoch of the solar system. When they are heated and expel this ancient material in their orbital motions around the Sun, we can have the opportunity to decipher the primitive information which have buried underneath the cometary surface for a long time. Herein, we present a brief overview of our observational results of a Jupiter-Family comet, 17P/Holmes, which underwent the historic outburst in 2007, to investigate its secular change in activity during 2014 perihelion passage. We performed the monitoring observation over two years, welcoming its first perihelion passage since the 2007 outburst. We analyzed the imaging data taken over two years, and found that there is a strong asymmetry of cometary activity with respect to the perihelion. Compared to the values taken right after the 2007 outburst, our results present a dust-production rate that has been utterly quenched by about five orders of magnitudes and is rather similar to that of pre-outburst inactive phase. We also found that the secular evolution of the fractional active area over the cometary surface had drastically dropped by about two orders of magnitudes in only one orbital revolution around the Sun. All of our results indicate that 17P/Holmes has entered upon an inactive phase far more rapidly than the prediction of the previous researches, and from this we conjecture that a surficial dust layer (~7 -10 cm in depth) of the comet play a dominant role as an insulator of sublimation of subsurface water ice from the solar irradiation.

Keywords: comets, 17P/Holmes

## DESTINY+: A Technology Demonstrator for Deep Space Exploration

\*Yasuhiro Kawakatsu<sup>1</sup>, Tomoko Arai<sup>2</sup>, Takahiro Iwata<sup>1</sup>, Tatsuaki Okada<sup>1</sup>, Ryu Funase<sup>3</sup>

1.ISAS, JAXA, 2.Planetary Exploration Research Center, Chiba Institute of Technology, 3.The University of Tokyo

DESTINY+, which stands for "Demonstration and Experiment of Space Technology for INterplanetary voYage," is a mission candidate for the next space science small program.

DESTINY+ is a high performance deep space transportation system whose maximum delta-v capacity is 5km/s, and maximum payload mass is 200kg. DESTINY is based on the previously developed small scientific standard satellite bus system, and extended by five novel technologies. The key technologies to realize DESTINY+ are, the large scale ion engine, the ultra-light weight solar panel, advanced thermal control devices, novel mission & orbit design, and small & high specification newly developed bus components.

DESTINY+ also demonstrate multiple fly-by explorations of near earth objects (NEO) by using instruments on DESTINY+ mother ship and its daughter probe "PROCYON mini". The first target NEO is one of the most unusual comet-asteroid transition bodies, 3200 Phaethon, which has dust tails. In this paper, we present the outline of mission plan, the system design, and key technologies of DESTINY+.

Keywords: DESTINY+, PROCYON-mini, Phaethon



## DESTINY+: Phaethon flyby with reUSable probe

\*Tomoko Arai<sup>1</sup>, Masanori Kobayashi<sup>1</sup>, Hiroki Senshu<sup>1</sup>, Koji Wada<sup>1</sup>, Ko Ishibashi<sup>1</sup>, Toshihiro Kasuga<sup>1</sup>, Manabu Yamada<sup>1</sup>, Shingo Kameda<sup>13</sup>, Katsuhito Ohtsuka<sup>3</sup>, Jun-ichi Watanabe<sup>2</sup>, Takashi Ito<sup>2</sup>, Yasuhiro Kawakatsu<sup>4</sup>, Sarli Bruno<sup>4</sup>, Takahiro Iwata<sup>4</sup>, Tatsuaki Okada<sup>4</sup>, Makoto Yoshikawa<sup>4</sup>, Tomoki Nakamura<sup>6</sup>, Hikaru Yabuta<sup>5</sup>, Sho Sasaki<sup>5</sup>, Mutsumi Komatsu<sup>7</sup>, Aiko Nakato<sup>4</sup>, Takahiro Hiroi<sup>8</sup>, Takashi Mikouchi<sup>9</sup>, Seitaro Urakawa<sup>10</sup>, Shinsuke Abe<sup>11</sup>, MASATERU ISHIGURO<sup>12</sup>, Hiroshi Kimura<sup>14</sup>, Shogo Tachibana<sup>15</sup>, Ryosuke Nakamura<sup>16</sup>, Keiko Nakamura-Messenger<sup>17</sup>, Mikiya Sato<sup>20</sup>, Ralf Srama<sup>18</sup>, Harald Kruger<sup>19</sup>

1.Planetary Exploration Research Center, Chiba Institute of Technology, 2.National Astronomical Observatory of Japan, 3.Tokyo Meteor Network, 4.JAXA, 5.Osaka University, 6.Tohoku University, 7.Sokendai, 8.Brown University, 9.The University of Tokyo, 10.Japan Spaceguard Association, 11.Nihon University, 12.Seoul National University, 13.Rikkyo University, 14.Kobe University, 15.Hokkaido University, 16.AIST, 17.NASA Johnson Space Center, 18.University of Stuttgart, 19.Max Planck Institutes, 20.Kawasaki Municipal Science Museum

Asteroid (3200) Phaethon is a parent body of the Geminids meteor shower. While most of the parent bodies of meteor showers are comets, cometary activity of Phaethon has only been reported near its perihelion at 0.14 AU. Phaethon is likely a comet to asteroid transitional body. Na depletion is reported from visible spectroscopic study of the ground observation of the Geminids meteoroid. Since an expected temperature by solar heating at 0.14 AU is not high enough to sublimate Na from Na-bearing phases, the observed Na depletion is likely derived from surface materials of the parent Phaethon. Na depletion does not occur in chondritic materials, but does occur in differentiated chondrites, such as primitive achondrites, which are subject to melting and segregation of Na-rich silicate melts. Phaethon may hold a signature of comet-asteroid transition body and primitive-differentiated material. Because of its small perihelion distance, dehydration of the surface material by solar heating is expected, but some primitive, hydrous material may still reside in its interior. Phaethon is an ideal body to understand on-going thermal evolution of primitive bodies in the solar system. Further, Phaethon is among the largest potentially hazardous asteroids (PHAs), of which cross the Earth's orbit. Thus, Phaethon is a critical mission target both in the context of science and planetary defense. Here, we present a flyby mission to Phaethon and its related asteroids by the DESTINY+mother ship and its daughter probe "PROCYON-mini", with their scientific significance.

Keywords: Asteroid (3200) Phaethon, Meteor Showers, Meteor shower parent bodies, Primitive bodies, DESTINY+, PROCYON-mini

## Size Dependence of Dust Distribution around the Earth Orbit

\*Takahiro Ueda<sup>1</sup>, Hiroshi Kobayashi<sup>2</sup>, Taku Takeuchi

1.Department of Earth and Planetary Sciences, Tokyo Institute of Technology, 2.Department of Physics, Nagoya University

In our solar system, there are many interplanetary dust particles (IDPs) originating mainly from asteroid collisions and activity of comets. These particles gradually decrease its angular momentum and drift radially due to the absorption and re-radiation of the sunlight (Poynting-Robertson effect; e.g. Burns et al. 1979). Investigating the properties of the zodiacal dust particles may reveal the properties of parent bodies and the creation process of them.

We analyzed the thermal emission from the IDPs called as the zodiacal light observed via all sky survey by the first Japanese infrared astronomical satellite, AKARI. We found that the observed surface brightness in the trailing direction of the Earth orbit is greater than that in the leading direction by 3.7% in band at 9 $\mu$ m and 3.0% in band at 18 $\mu$ m. This result is consistent with previous observations with IRAS (Dermott et al. 1994). This asymmetry is thought to come from the asymmetric dust distribution made by the IDPs trapped by MMRs of Earth orbit.

In order to reveal dust properties resulting in the asymmetry of dust distribution, we numerically integrated dust orbits in the Solar system including radiation from the Sun. The orbital evolution can be characterized by the parameter  $\beta$  which represents the strength of the radiation force compared to the gravitational force from the Sun. The parameter  $\beta$  can be defined as a function of dust properties such as dust radius  $s$  and material density  $\rho$ . In our calculations, particles are set to be 0.001-0.1 in  $\beta$  (corresponding to 3-300 $\mu$ m in radius with  $\rho = 2\text{g/cc}$ ) and their initial orbits are determined according to the origins of main-belt asteroids, Jupiter-family comets and Encke-type comets.

We found that larger particles are easier to be trapped by MMRs and make high density region in the dust distribution. However, larger particles are easier to be trapped by outer resonances which hardly contribute to the asymmetry in the surface brightness. In consequence, asteroidal grains of radius 30 $\mu$ m are most likely to make the asymmetry in the surface brightness. For cometary grains, due to the high eccentricity, particles are difficult to be trapped by resonance and less likely to make the asymmetry compared to the asteroidal grains.

In this presentation, we show the results of analysis of AKARI observations and orbital calculations and discuss the origin and typical size of the IDPs.

Keywords: Interplanetary dust particles, Earth

## Dynamical evolution of dust particles: from comets to the inner solar system

\*Hongu Yang<sup>1</sup>, MASATERU ISHIGURO<sup>1</sup>

1.Department of Physics and Astronomy Seoul National University ROK

There have been a long-standing debate regarding origins of interplanetary dust particles. Recent research about the optical properties and spatial distribution of zodiacal light suggested that ~ 90% of interplanetary dust particles which comprise the zodiacal light would be originated from comets. In this work, we started from different point of view. We studied the final status of dust cloud made by the dust particles ejected from comets. We chose representative comets which cover a wide variety of cometary orbital distribution. Hypothetical dust particles with different sizes were ejected from selected actual comets, following a dust ejection model based on cometary observations. We performed a numerical integration of dust orbits involving photon drag from solar radiation and perturbations from planetary gravitation. In this presentation, we will introduce our results about final positions of the cometary dust particles, and compare it with the observed quantities of interplanetary dust particles in the inner solar system, that is, the mass budget, size-frequency distribution, orbital elements distribution and zodiacal light brightness distribution.

Keywords: interplanetary dust particles, comets, zodiacal cloud, numerical simulation

## The MMX mission

\*Masaki Fujimoto<sup>1</sup>

### 1. Institute of Space and Astronautical Science, Japan Aerospace Exploration Agency

Martian Moons eXplorer (MMX) is the mission studied intensively by JAXA with the planned launch in 2022. It will explore the two moons of Mars, namely, Phobos and Deimos, and return samples from Phobos. The sampling will be done after detailed inspection of the moon from quasi-orbits around it is performed, while less detailed remote-sensing is planned for Deimos. The main objective of MMX is to understand the origin of the two Martian moons that remains controversial, with its goal being to reveal how small bodies at the outer-edge of the rocky-planet region behaved upon formation of the solar system. Mars is located at the outer-edge of the rocky-planet region, or at the gateway position to the snow line that demarcates the inner- and the outer-solar system. It is from beyond the snow line that water and volatiles were transported to the rocky planets. Without the across-the-snow-line transport, habitability is not an option for a rocky planet that was born dry inside the snow line. Small bodies, like those we find as primordial asteroids today, must have been the capsule for the transport, and thus, understanding the behavior of small bodies around the snow line during the formation of the solar system is one of the goals of planetary science as well as of MMX. In this talk, the mission scenario of MMX will be introduced and also discussed is the science strategy towards the mission goal via achieving its objectives.

## Observation of Mars in MMX mission

\*Takeshi Imamura<sup>1</sup>, Kazunori Ogohara<sup>2</sup>, Yasumasa Kasaba<sup>3</sup>, Shohei Aoki<sup>6</sup>, Makoto Taguchi<sup>4</sup>, Shingo Kameda<sup>4</sup>, Ichiro Yoshikawa<sup>5</sup>

1.Institute of Space and Astronautical Science, Japan Aerospace Exploration Agency, 2.Prefecture School of Engineering, The University of Shiga, 3.Department of Geophysics, Graduate School of Science, Tohoku University, 4.College of Science, Rikkyo University, 5.Department of Complexity Science and Engineering, The University of Tokyo, 6.Istituto di Astrofisica e Planetologia Spaziali, Istituto Nazionale di Astrofisica

To understand the water cycle and reservoir stability on Mars, investigation of localized water vapor transport and the diurnal cycle of phase change are important. Information obtained so far is quite limited because previous observations from polar, low-altitude orbiters did not obtain snapshots of high-resolution water vapor distribution and did not observe formation/evaporation of localized clouds. To understand dust lifting and the formation of global-scale dust distribution, investigation of fast, localized dust storms is important. Previous observations did not detect temporal development such events.

Observations of the Martian atmosphere in MMX from a high orbit will achieve a breakthrough via continuous, high-resolution global monitoring of dust, clouds, water vapor, and minor gases. The candidate instruments are mapping spectrometers in near-IR and UV, visible camera, and thermal IR camera. The expected outcomes are: spatial distribution of water vapor at fine scales; how water vapor emerges at specific locations, flows over long distances, and forms clouds; location, local time, and timescale of localized dust lifting; and how the lifted dust clouds spread and become diffuse.

Keywords: Mars, Atmosphere, MMX

## Key observations to understand the internal structure of Phobos

\*Hideaki Miyamoto<sup>1</sup>, Akito Araya<sup>2</sup>, Koji Matsumoto<sup>3</sup>, Naoki Terada<sup>4</sup>, Toshiyuki Nishibori<sup>5</sup>, Hiroshi Kikuchi<sup>1</sup>, Ryodo Hemmi<sup>1</sup>, Takafumi Niihara<sup>1</sup>, Hiroyuki Tanaka<sup>2</sup>, Kazunori Ogawa<sup>6</sup>

1.The University Museum, The University of Tokyo, 2.Earthquake Research Institute, University of Tokyo, 3.RISE Project Office, National Astronomical Observatory, 4.Graduate School of Science, Tohoku University, 5.JAXA, 6.Kobe university

Observations of Phobos by many spacecraft such as Viking orbiter, Mars Global Surveyor, Mars Odyssey, Mars Express, and Mars Reconnaissance Orbiter provided variety of datasets of the satellite including visible and color images, UV spectrum, global and high-resolution near IR and IR reflectance spectrum, radar reflectance, and precise orbiting parameters. However, because all of these missions have studied Phobos at distance, critical observations such as high-resolution imaging and precise gravity measurements have not been performed yet. In addition, Phobos exists in a very unique circum-Martian environment, which is significantly different from asteroids in the main belt. For example, impacts to Phobos should show the leading and trailing asymmetry due its synchronous rotation, which should also affect the deposition rates of re-impact of ejecta originated from Phobos itself. Also, the surface should have experienced space weathering due not limited to solar wind but also escape ions from Mars. Secondary impacts from Mars may contaminate the regolith of Phobos as well. Thus, understanding these processes is necessary to obtain a basic picture of surface evolution of the satellite. Important and necessary observations in the future mission would include (1) comprehensive mapping of craters and boulders, (2) study of sedimentary structures (if any) of regolith (layers) at high-resolution images, (3) high-resolution observations of geological features including grooves and depressions, (4) understanding of the degree of space weathering and its spatial distribution, and (5) a detection of dust ring on Phobos orbit.

The two distinctive color units observed on Phobos are interpreted in several ways, including an exposure of fresh internal materials over relatively weathered and totally different geological unit. In either case, their nature and understanding the surface processes would be important to derive information regarding its internal structure. Importantly, we do not know if an internal core exist or not, or even if the internal Ice exist (can vary from 0 to 60%). Also, the estimated bulk porosity can vary up to 70% and the surface materials may not represent the body. Therefore, key observations regarding the internal structure would include: (1) Detection of internal water-ice, which may be constrained by measurements of ion flux from inside, (2) Rough structure of the body in terms of gravity, (3) Shallow but precise subsurface structures including regolith thickness, contamination, layering, and the existence of base rock, which may be constrained by gradiometer observation, radar sounder, and lander's in-situ packages for porosity and particle size, (4) Exact density value at anywhere, which may be performed by Muography instrument.

Keywords: Phobos, internal structure, MMX

## The velocity and mass distributions of impact ejecta in the vicinity of the impact point: An application to the material transport from Mars to Phobos

\*Takaya Okamoto<sup>1</sup>, Kosuke Kurosawa<sup>1</sup>, Hidenori Genda<sup>2</sup>, Sunao Hasegawa<sup>3</sup>, Ayako Suzuki<sup>3</sup>, Koji Wada<sup>1</sup>, Takafumi Matsui<sup>1</sup>

1.Planetary Exploration Research Center, Chiba Institute of Technology, 2.Earth-Life Science Institute, Tokyo Institute of Technology, 3.Institute of Space and Astronautical Science, Japan Aerospace Exploration Agency

High-speed ejecta produced by a hypervelocity impact are transported to extremely far from the impact point. The surface of a satellite, Phobos, would contain Martian materials ejected by hypervelocity impacts (Ramsley and Head 2013). For understanding how much the ejecta can be transferred to Phobos, it is necessary to investigate the maximum velocity of impact ejecta and their mass in the vicinity of the impact point.

Although previous studies have been studied about the velocity distribution of impact ejecta from the position beyond the impactor's radius (e.g. Hermalyn and Schultz 2011, Tsujido et al., 2015), high-speed ejecta from just below the impact point have not been observed well. The ejection behavior has been also investigated using a numerical code in detail (Johnson et al., 2014). The simulation results, however, have not been validated through a comparison with the results of hypervelocity impact experiments.

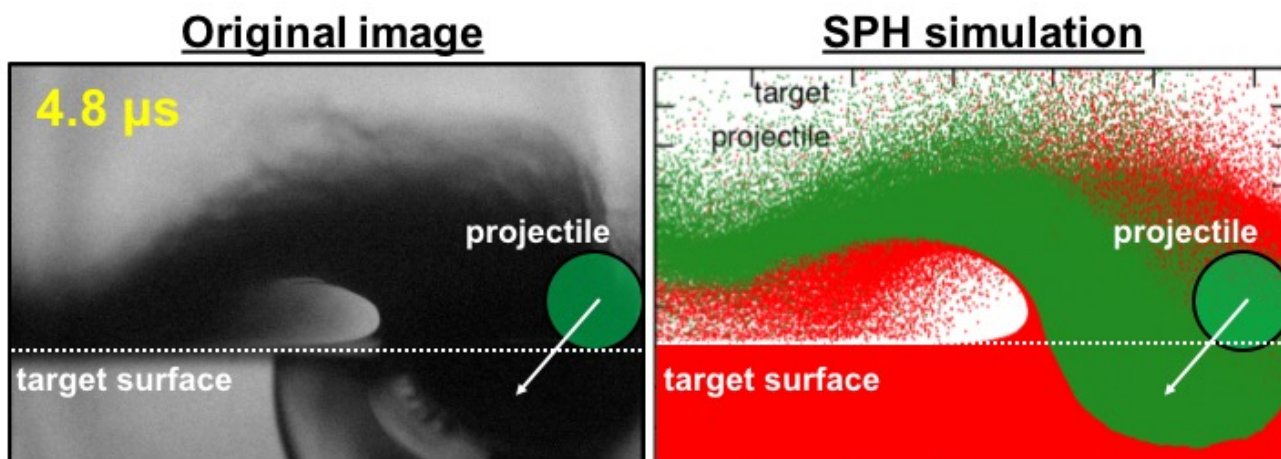
In this study, we performed impact experiments in order to observe the high-speed ejecta and to investigate the ejection velocity very near from the impact point using ultra-high-speed video camera. While the ejection velocity can be measured from the obtained images, it is difficult to determine the mass of the ejecta from impact experiments. We also performed SPH simulations of the impact ejecta in order to compare with the experimentally-observed ejection behavior under the same impact conditions, and to confirm the validity of the simulations. We investigated mass distribution of both target and projectile components in the ejected material in the simulations. We used polycarbonate as both projectiles and targets. Impact experiments were conducted using two-stage light gas guns at PERC/Chitech and ISAS/JAXA, Japan. Impact velocities were 3.56-7.04 km s<sup>-1</sup>. Impact angles were 90 degrees and 45 degrees measured from the target surface. High-speed video cameras (Shimadzu, HPV-X1, HPV-X2) were used, and the frame rate was 0.2  $\mu$ s frame<sup>-1</sup>, which enables us to observe the high-speed ejecta in the vicinity of the impact point because this time was much shorter than the time for a projectile penetration. The two cameras were used at ISAS/JAXA to observe the impact ejecta from two different directions in a right angle. This allows to reproduce three-dimensional images during impact processes.

Impact simulations were carried out with a three-dimensional SPH code (e.g. Genda 2012). The Tillotson EOS for polycarbonate was adopted (Sugita and Schultz 2003). We used 10<sup>4</sup>, 10<sup>5</sup>, and 10<sup>6</sup> SPH particles for a projectile to investigate the effects of the spatial resolution on the ejection behavior.

High-speed images show that a pattern of the ejecta curtain in the vertical impacts was almost axial symmetry like an umbrella. On the other hand, it was asymmetry in the oblique impacts, and two components of ejecta in different traveling directions were observed. One moved along the target surface to the downrange of the projectile trajectory. This is considered to be produced due to a jetting process during a projectile penetration (Kurosawa et al., 2015). The other component expands to the upward of the target surface. The boundary of the two component was observed as a kink. We confirmed that the SPH code with the highest spatial resolution, i.e., 10<sup>6</sup> SPH particles, reproduces the ejection behavior, including the travel distance of the outer edge of impact ejecta

and the two component in oblique impacts. The edge of the ejecta curtain consists of the target material during a vertical impact, whereas the leading edge of the ejected materials along the target surface is dominated by the projectile material during an oblique impact. We will discuss the application of the results to the problems of a material transport from Mars to Phobos.

Keywords: ejecta, hyper-velocity impact experiment, SPH simulation





## Origin and evolution of Phobos: Scientific objectives awaiting particle measurements by MMX

\*Naoki Terada<sup>1</sup>, Kanako Seki<sup>2</sup>, Yoshifumi Futaana<sup>3</sup>, Francois Leblanc<sup>4</sup>, Shoichiro Yokota<sup>5</sup>, Yoshifumi Saito<sup>5</sup>, Ayako Matsuoka<sup>5</sup>, Reiko Nomura<sup>5</sup>, Atsushi Yamazaki<sup>5</sup>, Junichi Kurihara<sup>6</sup>, Yayoi N. Miura<sup>7</sup>, Ken-ichi Bajo<sup>6</sup>, Ryuji Okazaki<sup>8</sup>, Tomoki Nakamura<sup>1</sup>, Shingo Kameda<sup>9</sup>, Yuichiro Cho<sup>9</sup>, science team MMX mission

1.Graduate School of Science, Tohoku University, 2.Graduate School of Science, The University of Tokyo, 3.Swedish Institute of Space Physics, 4.Laboratoire Atmospheres, Milieux, Observations Spatiales, 5.Institute of Space and Astronautical Science, Japan Aerospace Exploration Agency, 6.Graduate School of Science, Hokkaido University, 7.Earthquake Research Institute, The University of Tokyo, 8.Department of Earth and Planetary Sciences, Kyushu University, 9.School of Science, Rikkyo University

In this presentation, we will present scientific objectives of particle measurements by the Mars Moon eXploration (MMX) mission. The MINE (Magnetic field, Ion and Neutral Experiment) package consisting of five instruments (MSA, MIA, REN, NIMES, and MGF) and MEC (Mars Escaping atmosphere Capturing device) have been proposed as possible payloads of the MMX mission. MINE and MEC would perform particle measurements corresponding to the following three scientific objectives: (1) To obtain indirect information on the Phobos internal structure in order to constrain the origin of Phobos independent of the sample analysis results. (2) To characterize the space environment and the surface features of Phobos, with the intention of comparison with asteroids. (3) To constrain the total amount of atmosphere lost from Mars to space during its history. Details of these three scientific objectives will be presented.

Keywords: Phobos, Mars, Particle

## Gamma-ray and Neutron Emission from the Surface of Martian Moons

\*Masayuki Naito<sup>1</sup>, Hiroshi Nagaoka<sup>1</sup>, Kouhei Yoshida<sup>1</sup>, Junya Ishii<sup>1</sup>, Daisuke Aoki<sup>1</sup>, Hiroki Kusano<sup>2</sup>, Nobuyuki Hasebe<sup>1,2</sup>

1.School of Advanced Science and Engineering, Waseda University, 2.Research Institute for science and Engineering, Waseda University

Mars has two moons "Phobos" and "Deimos" which have never been explored. Japanese mission to Martian moons "Mars Moon eXploration (MMX)" is planned to obtain some evidences for determining the origin of Martian moons. This mission will pick up rock and soil sample from Phobos to the Earth to analyze in detail by laboratory techniques. There are two influential scenarios about the origin of the Martian moons, captured asteroid origin and giant impact origin. However, any previous studies have never succeed to explain the origin of the Martian moons completely.

The chemical composition of the Martian moons which is essential information for planetary science has not been observed before. Gamma-ray and Neutron Spectrometer (GNS) is proposed as one of the mission payloads in order to determine elemental compositions of two Martian moons by remote sensing. The captured asteroid origin indicates Martian moons of primitive chondritic composition which enriches with volatile elements (H, S) and depleted with Si and Ca [1]. On the other hand, Martian materials ejected by the giant impact made the moon if they have similar composition to Mars which is considered to be rich in Si and Ca [2]. Moreover, volatile elements are depleted because of evaporation by impact heat. Therefore, the ratios of Si/Fe, Ca/Fe and H concentration will be important indicators to give a constraint to the origin of Martian moons.

In this work, we have investigated gamma-ray and neutron emission depending on chemical composition and H concentration to support the potential to distinguish sample compositions by the GNS. The elemental composition of Martian meteorites and some types of chondrites were assumed as the giant impact origin and the captured asteroid origin, respectively. H concentration in these elemental compositions were varied in the range of 0-20000 ppm. Production and transportation of gamma-rays and neutrons produced by galactic cosmic rays (H and He; 10 MeV/n-100 GeV/n) were calculated by using the Monte Carlo simulation code PHITS (Particle and Heavy Ion Transport code System) [3] and the INCL (Intra Nuclear Cascade of Liège) nuclear interaction model [4].

The Si/Fe and Ca/Fe ratios of gamma-rays emitted from Martian composition showed high values while that from chondrite composition showed low values. There are some differences in the shape of neutron energy spectra between Martian and chondritic samples. The neutron energy spectrum from chondrite shows a peak at the energy range of thermal neutron < 0.5 eV and a low flux of epithermal neutron energy from 0.5 eV to 500 keV comparing to that from Martian meteorite. In contrast, the shapes of fast neutron flux > 500 keV almost correspond. It is considered that the differences of H concentration in the sample composition caused this differences in neutron spectra since H atoms moderate neutrons effectively. The neutron fluxes were significantly varied depending on H concentration. Fast and epithermal neutron fluxes decreased with H concentration while thermal neutron flux increased until 2000 ppm of H and decreased above the value. Epithermal neutron flux is effective to determine H concentration since the change of epithermal neutron was larger than that of thermal and fast neutrons. By combining the ratios of Si/Fe and Ca/Fe and H concentration determined by gamma-rays and neutrons, the GNS will give an important constraint to the origin of the Martian moons.

The simulation results of the Martian moons will be presented and discussed.

[1] E. Jorosewich, *Meteoritics* 25 (1990) 323.

[2] NASA Martian meteorite Compendium, <http://curator.jsc.nasa.gov/antmet/mmc/>.

[3] T. Sato et al., *J. Nucl. Sci. and Technol.* 50 (2013) 913.

[4] A. Boudard et al., *Phys. Rev.* C87 (2013) 014606.

Keywords: Gamma-ray and Neutron Spectrometer, Martian moons, GNS

## On the origin of Martian moons

\*Hidenori Genda<sup>1</sup>, Ryuki Hyodo<sup>2,3</sup>, Sebastien Charnoz<sup>3</sup>, Pascal Rosenblatt<sup>4</sup>

1.Earth-Life Science Institute, Tokyo Institute of Technology, 2.Kobe University, 3.IPGP, 4.Royal Observatory of Belgium

We will review the origin of Martian moons with our recent works. We will also present the science aspects of the MMX mission.

Keywords: sample return, Martian moons, origin

## Development of near- and mid-infrared imaging spectrometers for the Martian moon's sample return mission and next generation space projects

\*Takeshi Sakanoi<sup>1</sup>, Takahiro Iwata<sup>2</sup>, Tomoki Nakamura<sup>4</sup>, Yasumasa Kasaba<sup>4</sup>, Makoto Taguchi<sup>5</sup>, Hiromu Nakagawa<sup>4</sup>, Masato Kagitani<sup>1</sup>, Atsushi Yamazaki<sup>2</sup>, Shohei Aoki<sup>3</sup>, Takao M. Sato<sup>2</sup>

1.Planetary Plasma and Atmospheric Research Center, Graduate School of Science, Tohoku University, 2.JAXA, ISAS, 3.Istituto di Astrofisica e Planetologia Spaziali, INAF, 4.Graduate School of Science, Tohoku University, 5.College of Science, Rikkyo University

We report the current design of near-infrared spectrometer for the MMX (Mars Moon eXploration) mission, and also discuss near- and mid-infrared spectroscopy for next generation space projects with advanced imaging technology. MMX spacecraft is scheduled to be launched in the early 2020s, orbits Phobos and Deimos, and returns samples from Phobos back to Earth in the late 2020s. Near-infrared spectroscopy is useful to understand the material distribution on Martian moons (e.g., hydroxide minerals at 2.7–2.8  $\mu\text{m}$ , hydrated minerals at 3.0–3.2  $\mu\text{m}$ , and organics at 3.4–3.4  $\mu\text{m}$ ) and dynamics in Martian atmosphere (e.g. H<sub>2</sub>O at 2.5–2.65  $\mu\text{m}$ , and pressure with CO<sub>2</sub> absorption at 1.2–2.2  $\mu\text{m}$ ). We proposed a near-infrared spectrometer NIRS4 for the MMX mission to carry out the near-infrared spectroscopic measurement of the Martian moons Phobos and Deimos and Martian atmosphere. NIRS4 is based on the NIRS3 on the Hayabusa-2 spacecraft, which has a fast optics (F-number 1.4) with a long slit corresponds to a wide field-of-view (FOV) of 14.6 x 0.03 deg. NIRS4 covers the target area of 26 km length with 100 m spatial resolution looking from 100 km altitude. It also achieves 20 m and 1 m spatial resolution, respectively, from altitudes of 20 km and 1km. A grism is put in the collimating optics, and its wavelength resolution is ~ 1.5 to 3 nm (R~650 to 1000). A 2D HgCdTe array (640 x 512 pixel, pixel size 15 x 15 microns, sensitivity range 1–3.8 microns) is used as a detector. The detector and optical system are cooled down below 90 K and 190 K with a Stirling cooler to reduce thermal noise. As an order sorter of dispersion light, we put 1–1.9  $\mu\text{m}$  (1<sup>st</sup> order) filter on a half part of the slit, and 1.9–3.8  $\mu\text{m}$  (2<sup>nd</sup> order) filter on the other half of the slit. In this way, a half FOV (7.3 x 0.03 deg) with wavelength range of 1–1.9  $\mu\text{m}$  is focused on a half side of 2D detector (640 x 256 pixel area), and the other half FOV with wavelength of 1.9–3.8  $\mu\text{m}$  is focused on the other half of the detector. The calibration lamp is used to determine the absolute wavelength. An optical chopping system which periodically interrupts an incident light to determine the background level precisely and to gain the signal-to-noise ratio.

Keywords: Mars, MMX, near-infrared spectrometer

## Deployable Camera system 5 (DCAM5) proposed for Martian Moon Exploration mission (MMX)

\*Koji Wada<sup>1</sup>, Hirotaka Sawada<sup>2</sup>, Kazunori Ogawa<sup>3</sup>, Kei Shirai<sup>2</sup>, Naoya Sakatani<sup>2</sup>, Ko Ishibashi<sup>1</sup>, Rie Honda<sup>4</sup>, Minami Yasui<sup>3</sup>, Masahiko Arakawa<sup>3</sup>

1.Planetary Exploration Research Center, Chiba Institute of Technology, 2.ISAS/JAXA, 3.Kobe Univ., 4.Kochi Univ.

We propose Deployable Camera system 5 (DCAM5) for remote and in situ observations of Phobos and Deimos in Martian Moon Exploration mission (MMX) led by JAXA. DCAM5 is the latest version of the DCAM series in space missions (DCAM1 and 2 were successfully operated in IKAROS mission and DCAM3 is equipped on Hayabusa2 mission). In this mission MMX, DCAM, a small handy-sized body equipped with several visible cameras, a triaxial accelerometer, batteries, and a communication unit will be separated from the spacecraft (SC) and thrown toward scientifically valuable regions of Phobos and Deimos where SC cannot approach nor land on, e.g., inner wall of Stickney crater.

As falling toward a target region, DCAM will take multiscale, multiband images of the target regions with a multiband camera equipped on the leading edge of DCAM. Multiband images with high resolutions down to  $\sim 1$  cm/pix will reveal spectroscopic characteristics of the target region, such as the distribution of hydrated minerals and the texture of boulders which could reflect the thermal evolution of Phobos and Deimos. When DCAM collides to Phobos surface, we will measure the acceleration profiles at collision as an indicator of the mechanical properties of the landing point. From the acceleration profiles we will obtain the following properties depending on the nature of the landing point: (1) in the case of landing on a boulder, disruptive strength of boulders, which allows us to estimate  $Q^*$  value reflecting the thermal evolution of Phobos, (2) in the case of landing on a regolith layer, penetration resistance (drag coefficient) of regolith layers which allow us to constrain the surface evolution inherent to Martian moons, and (3) in the case of a fine powder layer, compression curves of powder layers which reflects the porosity and the cohesion of the layer, constraining the levitation process on small bodies and the compression evolution of fluffy bodies such as planetesimals. After landing of DCAM, we will take close-up images of the surface to clarify the size and the porosity of the surface regolith.

Since DCAM is a light and small body, several DCAMs are preferred to be equipped and thrown toward different, valuable regions to reveal the origin and the evolution of Phobos and Deimos. Furthermore, we propose two objectives of DCAM5 other than the described above: one is to investigate candidate landing points on Phobos before landing of SC and the other is to observe the status of SC at around its landing and the disturbance of the landing points. Since each objective is achieved with one or more DCAMs, we need 3 DCAMs at least in order to complete all the objectives.

Keywords: Martian moons, planetary exploration, onboard instrument , DCAM

## Geophysical experiments on Phobos proposed for JAXA Mars Moon Exploration mission

\*Kazunori Ogawa<sup>1</sup>, Satoshi Tanaka<sup>2</sup>, Naoya Sakatani<sup>2</sup>, Munetaka Ueno<sup>1,2</sup>, Takeshi Hoshino<sup>2</sup>, Kazutoshi Sakamoto<sup>2</sup>, Taichi Kawamura<sup>3</sup>, Yoshiaki Ishihara<sup>2</sup>, Nozomu Takeuchi<sup>4</sup>, Philippe Lognonné<sup>3</sup>, Akito Araya<sup>4</sup>, Ryuhei Yamada<sup>5</sup>, Takeshi Tsuji<sup>6</sup>, Taizo Kobayashi<sup>7</sup>, Kei Shirai<sup>8</sup>, Matthias Grott<sup>9</sup>, Jerzy Grygorczuk<sup>10</sup>, Axel Hagermann<sup>11</sup>, Jörg Knollenberg<sup>9</sup>, Tilman Spohn<sup>9</sup>, Hideaki Miyamoto<sup>4</sup>, Hiroaki Katsuragi<sup>12</sup>, Sin-iti Shirono<sup>12</sup>, Tomokatsu Morota<sup>12</sup>, Masahiko Arakawa<sup>1</sup>

1.Kobe University, 2.Japan Aerospace Exploration Agency, 3.Institut de Physique du Globe de Paris, 4.University of Tokyo, 5.National Astronomical Observatory of Japan, 6.Kyushu University, 7.University of Fukui, 8.The Graduate University for Advanced Studies, 9.German Aerospace Center, 10.Polish Academy of Sciences, 11.Open University, 12.Nagoya University

Scientific instruments and their support devices are being proposed for geophysical experiments on Phobos as potential instruments for the Mars Moon Exploration mission (MMX). JAXA is currently planning a sample return mission to the martian moons. The spacecraft will stay in a quasi-orbit around Phobos for months or 1-2 years, and make scientific observations including remote sensing, landings on Phobos for sampling, and several flybys of Deimos. Scientific goals of MMX were defined as in the following two categories: (1) To reveal the origin of the Mars moons, and then to make a progress in our understanding of planetary system formation and of primordial material transport around the border between the inner- and the outer-part of the early solar system. (2) To observe processes that have impact on the evolution of the Mars system from the new vantage point and to advance our understanding of Mars surface environment transition. While a landing site for sampling is still under consideration, in a current plan the main spacecraft lands twice, on the "red" and "blue" areas on Phobos for example.

We proposed five scientific instruments for this mission. SEIS: a three-axes short-period seismometer and an active seismic vibration source, SSXT: a penetration probe of several tens cm length with temperature and thermal conductivity sensors, miniRAD: a miniaturized thermal infrared radiometer, a muon detector, and SUMIRE: a mechanical insertion resistance probe of 5 cm length. All these instruments basically aim at investigating the geophysical properties of the surface, sub-surface, and interior of Phobos, and their combined observations can provide integrated models of mechanical and thermal properties of the subsurface which has not been studied so far. The scientific objectives of these instruments are connected to the following mission objectives corresponding to the mission goals above: (a) To obtain indirect information on the Phobos internal structure in order to constrain the origin of Phobos independent of the sample analysis results. (b) To characterize the space environment and the surface features of Phobos, with the intention of comparison with asteroids.

Because the first four of the above scientific instruments require a long observation time at a fixed location, a long-lived landing package (MSM) is also proposed. SUMIRE is planned to be mounted on the feet of the mothership (main lander). Objectives of MSM are providing electric power, command/telemetry interfaces, and an operable environment for the scientific instruments throughout a period of our observations over a Mars year. MSM has the following specifications and functions: (i) Operates independently from the mothership and survives at a fixed point of area. (ii) Controls internal temperature in an operable range of the scientific instruments for their continuous observations. (iii) Provides wired interfaces of telemetry/command and power to the scientific instruments. (iv) Communicates over a radio link with the mothership in orbits and with ground-based stations on the Earth. MSM will be placed on Phobos' surface during the landing sequence of the main spacecraft, and stay there over its entire lifetime.

Keywords: MMX, Martian moon, Phobos, Planetary exploration, Internal structure



## Moments of inertia of Phobos with inhomogeneous internal structure

\*Koji Matsumoto<sup>1</sup>, Hitoshi Ikeda<sup>2</sup>

1.RISE Project Office, National Astronomical Observatory, 2.RDD/JAXA

The origin of Phobos is still an open issue. It may be either captured asteroid or formed from a disk of impact ejecta produced by a giant impact. Although it is not straightforward to determine the origin from internal structure alone, it will place important constraints. One of the key parameters related to the internal structure is moments of inertia (MOI). Phobos's MOI can be determined from amplitude of short-period forced libration and degree 2 gravity coefficients. Currently, the libration amplitude is estimated to be  $1.09 \pm 0.01$  degrees by analyzing multiple image data [1]. Although the degree 2 gravity coefficients are estimated from tracking data of Mars Express on its close flyby at Phobos, they are not solved for at sufficient accuracy [2]. Axial difference of MOI can be constrained by the libration amplitude, but currently MOI of Phobos is not known. The observed libration amplitude is consistent with homogenous mass distribution of Phobos, but local mass anomalies cannot be ruled out [1, 3]. Here we consider relatively simple two-layer internal structure and assume that ice water or porosity is confined in either layer, and calculate how much MOI deviate from the value for homogeneous body if such an inhomogeneity existed. Phobos's bulk density of  $1.86 \pm 0.013$  g/cm<sup>3</sup> [4] is lower than most of the samples of carbonaceous material, which requires porosity and/or light elements like water ice. If the low bulk density was explained by water ice, its mass fraction is expected to be 10-35% depending on rocky material grain density [5]. If the mass distribution inside Phobos was inhomogeneous, e.g., water ice was concentrated near the surface or the center, we will observe a deviation of MOI from the value for homogenous interior. Here the MOI differences (dMOI) with respect to the homogenous Phobos are calculated for some cases where we assumed that (1) Phobos has a tri-axial ellipsoidal figure ( $a = 13.03$  km,  $b = 11.40$  km,  $c = 9.14$  km), (2) Phobos has a two-layer structure and their boundary also has the similar ellipsoidal figure for which the libration amplitude is 1.15 degrees being consistent with the observed value of [1], and (3) water ice is confined either of the upper or lower layer and rock density is the same for both the layers. The water ice mass fraction is changed between 0 and 30% .

In the case that upper layer is composed of the rock plus water ice, when the upper layer thickness is 10% of the semi-principal axes, no more than 14 wt.% of water can be contained in the layer and the maximum dMOI is about 9%. When the layer boundary is deeper, more water can be contained, but the maximum dMOI is about 16%. In the case that the water ice is confined in the lower layer, the maximum dMOI is also about 17%.

We also tested the cases in which the porosity is responsible for the low bulk density. We calculated due to inhomogeneous distribution of the porosity using the similar two-layer structure. The results depend on the boundary depth and rock density. In the case that the lower layer is porous, the maximum dMOI is about 17% when rock density is 2400 kg/m<sup>3</sup>, and about 9% when rock density is 2100 kg/m<sup>3</sup>.

It is found that, for the layer configuration assumed here, dMOI is smaller than 16-17%. A 10% accuracy will not be sufficient, and it is required to achieve at least a few percent of MOI accuracy in order to detect it. To this end, the required accuracies for the libration amplitude and the degree 2 gravity coefficients are also a few percent.

References:

[1] Oberst et al. (2014) *Planet. Space Sci.*, 102, 45-50.[2] Pätzold et al. (2014) *Icarus*, 229, 92-98.

- [3] Rambaux et al. (2012) *Astron. Astrophys.*, 548, A14.
- [4] Willner et al. (2014) *Planet. Space Sci.*, 102, 51-59.
- [5] Rosenblatt (2011) *Astron. Astrophys. Rev.*, 19 (44).

Keywords: Phobos, internal structure , moments of inertia

## Topographic degradation of craters on the moon of Mars, Phobos

\*Seiya Morita<sup>1</sup>, Tomokatsu Morota<sup>1</sup>, Sei-ichiro Watanabe<sup>1</sup>

1. Graduate School of Environmental Studies, Nagoya University

The origin of the two Mars satellites Phobos and Deimos is controversial and evolution thereafter is also unclear. A numerical study showed that nearly all impact fragments ejected from the inner moon Phobos remain trapped in Mars orbits until re-impact with Phobos and produce new generations of ejecta. The suggesting process seems consistent with the observed thick regolith of Phobos. Such re-accumulation may also affect the shape of craters on Phobos. Thus, the crater morphology is expected to give us a key to read out the geological history of this enigmatic satellite. Contrary to rimmed craters on the Moon, craters on the low-gravity satellite Phobos have no clear rims, so that a new method of crater morphology applicable to low-gravity satellites should be developed. On the Moon, the degradation of craters is controlled by the accumulation of smaller later impacts and follows topographic diffusion process. However, old lunar craters tend to be inconsistent with topographic diffusion model because ejecta deposits of larger later impacts effect crater degradation. On the Phobos, on the other hand, the crater degradation is expected to be consistent with topographic diffusion model in the longer time scale than that on the Moon because impact fragments spread all over the Phobos surface and large later impacts have a smaller effect on the shape of craters than the Moon.

So, I propose a crater shape analysis based on a topographic diffusion model, applicable to craters on a small body, and estimate the model ages of Phobos craters from the degree of crater degradation. I made averaged topographic profiles of twenty craters with radii larger than 1km and compared each of them with a diffusion-model profile having the same flexion-point radius. I find that the topographic profiles of most of the craters are consistent with corresponding diffusion profiles. Further, in each crater, the maximum angle of slope is proportional to depth normalized by the flexion-point radius, which is consistent with the prediction of the topographic diffusion model, and the model age  $kt$  (where  $k$  is the topographic diffusivity and  $t$  is the crater age) can be determined. The distribution of  $kt$  of the craters is, however, concentrated in lower values, which is inconsistent with the topographic diffusion model with  $k$  correlated to crater-forming impact flux. These results suggest that Phobos experienced some unique erosion process incompatible with simple topographic diffusion models.

Keywords: Phobos, crater, degradation

## Geological investigation of the blue unit on Phobos

\*Hiroshi Kikuchi<sup>1</sup>, Hideaki Miyamoto<sup>1</sup>, Ryodo Hemmi<sup>1</sup>

1.The University Museum,The University of Tokyo

The surface of the Martian satellite, Phobos, is spectrally divided into two units: red and blue. Understanding their difference may be key to determining the origin and evolution of Phobos, because the blue unit has commonly been interpreted to be composed of original materials of Phobos. Whereas the red unit is distributed nearly globally, the blue unit maps to some relatively small impact craters and the largest crater on Phobos, ~ 9 km-diameter Stickney crater, and its nearby surroundings. Hypotheses to explain its distribution include: (1) emplacement of low-velocity ejecta from the Stickney impact [1], (2) landslide materials extending to the west of Stickney crater [2], and (3) an inner heterogeneous structure of Phobos [e.g., 3; 4]. Regarding (1), Thomas 1998 suggests that low-velocity Stickney ejecta are capable of distributing asymmetrically due to the effects of Phobos' rapid spin, however the emplacement velocity did not be considered. The ejecta may have been emplaced beyond the extent hypothesized. Using high-resolution images, we investigate this with high precision.

We examine the largest region of the blue unit east of Stickney by: changing the NIR/BG color ratio for the western part of HiRISE (High Resolution Imaging Science Experiment) images based on the analysis of [5]. In order to compare these maps, we create a dynamical potential map by dividing the numerical shape model [6] into 1,672,215 small triangular pyramid. From the tidal, centrifugal, and self-gravitational forces [7], we calculate the dynamical potentials at 121,770 points on the surface of Phobos. In addition, we perform numerical simulations in order to examine the relationships between the patterns of Stickney ejecta and regions of blue unit. Considering the rotation of Phobos, as well as the gravity of Phobos and Mars, we map the emplacement where the simulated orbit of particles and the sphere of Phobos intersect and calculate the emplacement velocities based on our simulations. In the calculation of the potentials and the simulations, we change values of the distance between Phobos and Mars from 20,000 km to 9,376 km to account for the changing distance through time. Moreover, we calculate the angle and the direction of the potentials.

As a result, many blue materials exist on the floor of craters and grooves. Comparing the spatial extent of the blue unit in the region east of Stickney crater to the slope map, a greater occurrence of the blue unit is observed on gentle slopes with increasingly less occurrence with greater slope angle. When performing comparative analysis among the maps generated based on varying orbital distances, the extent of the blue unit appears to be consistent with the current orbit. From our simulations, the emplacements of low velocity ejecta of Stickney cover one of blue unit regions east of Stickney.

Our results suggest that blue material easy to move rather than red material. Moreover if the origin of materials composing the blue unit is ejecta of an impact crater of Phobos, the emplacement velocity of the ejecta deposits must be lower than the escape velocity of Phobos. Based on these investigations, we interpret that the Stickney crater is underpinned by the blue unit with its surface being modified into the ubiquitous red unit through space weathering among other processes. Subsequently, the impact event except for Stickney might expose fresh blue materials.

[1] Thomas P. C. (1998) *Icarus*, 131, 78-106. [2] Shingareva T. V. and Kuzmin R. O. (2001) *Sol. Syst. Res*, 35, 431-443. [3] Murchie S. et al. (1991) *JGR*, 96, 5925-5945. [4] Basilevsky A. T. et al. (2014) *PSS*, 102, 95-118. [5] Thomas N. et al. (2011) *PSS*, 59, 1281-1292. [6] Gaskell R.W. (2011) Gaskell Phobos Shape Model V1.0. V01-SA-VISA/VISB-5-PHOBOSHAPE-V1.0. NASA Planetary Data

System. [7] Thomas P. C. (1993) *Icarus*, 105, 326-344.

Keywords: Phobos, Blue unit, Stickney crater

## Solids and Fluids of volatile (carbon)-bearing materials on Asteroids and Martian Moons

\*Yasunori Miura<sup>1</sup>

## 1. Visiting (Yamaguchi, In &amp; Out Universities)

## Introduction

Asteroids and Moons (of Earth and Mars) are studied mainly from material sciences of mineral and texture with formation ages by using database of Earth' rocks and collected meteorites (Asteroids and Earth's Moon), where the collected meteorites show quenched texture and limited mineral-solids without remained fluids. The main purposes of the paper is to elucidate formation processes of solids and fluids of Asteroids and the Moons.

## Solidified fluids on meteorites:

Remained fluid-water cannot be obtained at meteorites and Moon (Earth) rocks, because global water (on Earth) with formation of many mineral series and rock kinds cannot be confirmed. Fluid formation of these meteorites are rapidly solidified to be formed groundmass among chondrules and/or phenocryst of crystalline minerals. This indicates that fluids are formed quickly and changed to non-crystalline aggregates to fix solids of chondrule crystalline grains from meteorite texture.

## Solidified micro-grains produced by laser melting:

Author has produced quick fluids texture during laser sputtering experiments of carbon-bearing rocky grains in this study. This indicates formation of fluid liquid phase from solid mineral to quenched grains though there are no previous fluid water in the sample before laser sputtering process..

Similar heating experiment of carbonaceous meteorite produces only water after heating reaction though there are no water before heating.

The present experimental results indicate that there are any elements, ion and elements of fluids (water and carbon dioxides) are existed separately and combined by extreme conditions of high temperature and pressure, which can explain clearly the poor mineral and rock kinds compared with water-planet showing circulated fluids and water supply by interior activity.

Carbon-bearing materials formed at collisions on asteroids.

Almost all evaporated elements are disappeared without any remained solidified materials (except carbon-bearing grains) after impacted collision on Asteroid surface. In fact, we can observed solidified carbon-bearing nano-grains on the Moon rocks (Africa and Antarctica) and chondritic meteorites (ordinary to carbonaceous samples), which indicate that the Moons and any Asteroids have volatile carbon-bearing materials on the surfaces.

## Expected space explorations for the Moons and Asteroids:

Among many Asteroids, volatile (carbon)-bearing materials are produced for active multiple collisions (including impact crater sites) or largely broken small bodies by huge collision, where many material resources with volatiles (carbon and/or hydrogen) are expected to be find for next human resources on space world in future.

## Summary:

Natural resources of volatile (carbon)-bearing materials on the two Moons (Mars) and Asteroids are expected for next target for sample collection and material circulation sites for limited living bases in future, which are obtained by meteorite analyses and artificial laser experiments.

Keywords: Solids and Fluids , Volatile (carbon)-bearing materials , Asteroids and Martian Moons



## Gravity science investigation of Ceres from Dawn

\*Ryan Park<sup>1</sup>

1.Jet Propulsion Laboratory, California Institute of Technology, Pasadena, CA, USA, 2.IMCCE, Observatoire de Paris, Paris, France, 3.Massachusetts Institute of Technology, Cambridge, MA, USA, 4.Lamont-Doherty Earth Observatory, Columbia University, Palisades, NY, USA, 5.University of Toulouse, Toulouse, France, 6.UCLA, Los Angeles, CA, USA.

R.S. Park<sup>1</sup>, A.S. Konopliv<sup>1</sup>, B.G. Bills<sup>1</sup>, N. Rambaux<sup>2</sup>, J.C. Castillo-Rogez<sup>1</sup>, C.A. Raymond<sup>1</sup>, A.T. Vaughan<sup>1</sup>, A. Ermakov<sup>3</sup>, M.T. Zuber<sup>3</sup>, R. Fu<sup>4</sup>, M.J. Toplis<sup>5</sup>, C.T. Russell<sup>6</sup>, <sup>1</sup>Jet Propulsion Laboratory, California Institute of Technology, Pasadena, CA, USA (e-mail Ryan.S.Park@jpl.nasa.gov); <sup>2</sup>IMCCE, Observatoire de Paris, Paris, France; <sup>3</sup>Massachusetts Institute of Technology, Cambridge, MA, USA; <sup>4</sup>Lamont-Doherty Earth Observatory, Columbia University, Palisades, NY, USA; <sup>5</sup>University of Toulouse, Toulouse, France; <sup>6</sup>UCLA, Los Angeles, CA, USA.

The Dawn gravity science investigation utilizes the DSN radiometric tracking of the spacecraft and on-board framing camera images to determine the global shape and gravity field of Ceres. The gravity science data collected during Approach, Survey, and High-Altitude Mapping Orbit phases were processed. Currently, the latest gravity field called CERES08A is available, which is globally accurate to degree and order 5. Combining the gravity and shape data gives the bulk density of  $2163 \pm 8 \text{ kg/m}^3$ . The low Bouguer gravity at high topography area, or vice versa, indicates that the surface of Ceres is likely compensated and that its interior presents a low-viscosity layer at depth. The degree 2 gravity harmonics show that the rotation of Ceres is very nearly about a principal axis. This is consistent with hydrostatic equilibrium at the 3% level. This infers that the mean moment of inertia of Ceres is , implying some degree of central condensation. Based on a simple two-layer model of Ceres and assuming carbonaceous chondrites and hydrostatic equilibrium, the core size is expected to be ~280 km with corresponding average thickness of the outer shell of ~190 km and density of  $\sim 1950 \text{ kg/m}^3$ .

Keywords: Ceres, Dawn, Dwarf planet



The Instrument error on estimation of normal albedo of Ryugu using the laser altimeter on-board Hayabusa2 and the reflectance measurement of the carbonaceous chondrite at zero phase angle

\*Ryuhei Yamada<sup>1</sup>, Hiroki Senshu<sup>2</sup>, Noriyuki Namiki<sup>1</sup>, Takahide Mizuno<sup>3</sup>, Shinsuke Abe<sup>4</sup>, Fumi Yoshida<sup>1</sup>, Kazuyoshi Asari<sup>1</sup>, Hiroto Noda<sup>1</sup>, Naru Hirata<sup>5</sup>, Shoko Oshigami<sup>1</sup>, Hiroshi Araki<sup>1</sup>, Yoshiaki Ishihara<sup>3</sup>, Koji Matsumoto<sup>1</sup>

1.National Astronomical Observatory of Japan, 2.Chiba Institute of Technology, 3.Japan Aerospace Exploration Agency, 4.Nihon University, 5.The University of Aizu

The Japanese asteroid explorer 'Hayabusa2' was launched at end of 2014 to explore the near-Earth C-type asteroid 'Ryugu'. In this mission, we have a plan to apply the laser altimeter (LIDAR) on-board Hayabusa2 to investigate the distribution of normal albedo of Ryugu at a laser wavelength (1064 nm). The LIDAR instrument for laser ranging which has a function to measure the intensities of transmitted and received pulses. The intensities data can be used to estimate the normal albedo of Ryugu.

In this study, we evaluated the contribution of the instrument error to the normal albedo uncertainty on the estimation from the intensities data. From the evaluation, we found the error due to instrument effects was 18% at an altitude of 20 km based on the verification tests of the LIDAR flight model. The surface slope and roughness elongate the time width of the returned pulse and decrease the intensity. We will also describe how the returned pulse is deformed as a result of slope and roughness.

Currently, we prepare for reflectance measurement of the carbonaceous chondrites at observation condition of the LIDAR to obtain calibration data to interpret the normal albedo variation on Ryugu. In this experiment, we enabled measurement of the reflectance at zero phase angle and wavelength of 1064 nm using a beam splitter. Then, to compare and integrate the normal albedo estimated from the LIDAR data with the reflectance data measured by other instrument equipped on Hayabusa2 (the optical camera and near-infrared spectrometer), the phase angles can be controlled from 0 to 30 degrees on the experiment. In this presentation, we will report configuration of the reflectance measurement and preliminary results.

Keywords: Asteroid albedo, Ryugu, Hayabusa2, Laser altimeter, Carbonaceous chondrite, Reflectance measurement

## The origin of Itokawa dimples and a comparison with the surface structure of Phobos

\*Masato Kiuchi<sup>1</sup>, Akiko Nakamura<sup>1</sup>

## 1. Graduate School of Science, Kobe University

High-resolution images of asteroid 25143 Itokawa obtained by Hayabusa mission revealed that the surface of Itokawa has unique feature compared to other asteroids. The surface of Itokawa can be divided into two regions, one is rough terrain composed by many boulders and the other is smooth terrain composed by fine materials. On the smooth terrains small dimples associated with boulders are observed. This structure was considered as results of low-velocity impacts of boulders (Nakamura et al., 2008) or seismic shaking beneath boulders (Hirata et al., 2009), however, the origin of dimples have not been understood.

Although widely used successfully for craters on planetary surfaces, whether the scaling law about crater size (Holsapple, 1993) can be applied to low-velocity impacts is not obvious. This scaling law was originally derived based on point source approximation which can be applied when the crater size is sufficiently large as compared with impactor size. Moreover, the gravity dependence of crater diameter has not been fully understood. Hypervelocity impact experiments were conducted under increased gravities (Schmidt and Housen, 1987) and under low gravities (Gault and Wedekind, 1977). In these experiments crater diameter was proportional to about  $-0.17$  power of gravitational acceleration. However, there are few impact experiments under different gravity condition except above experiments.

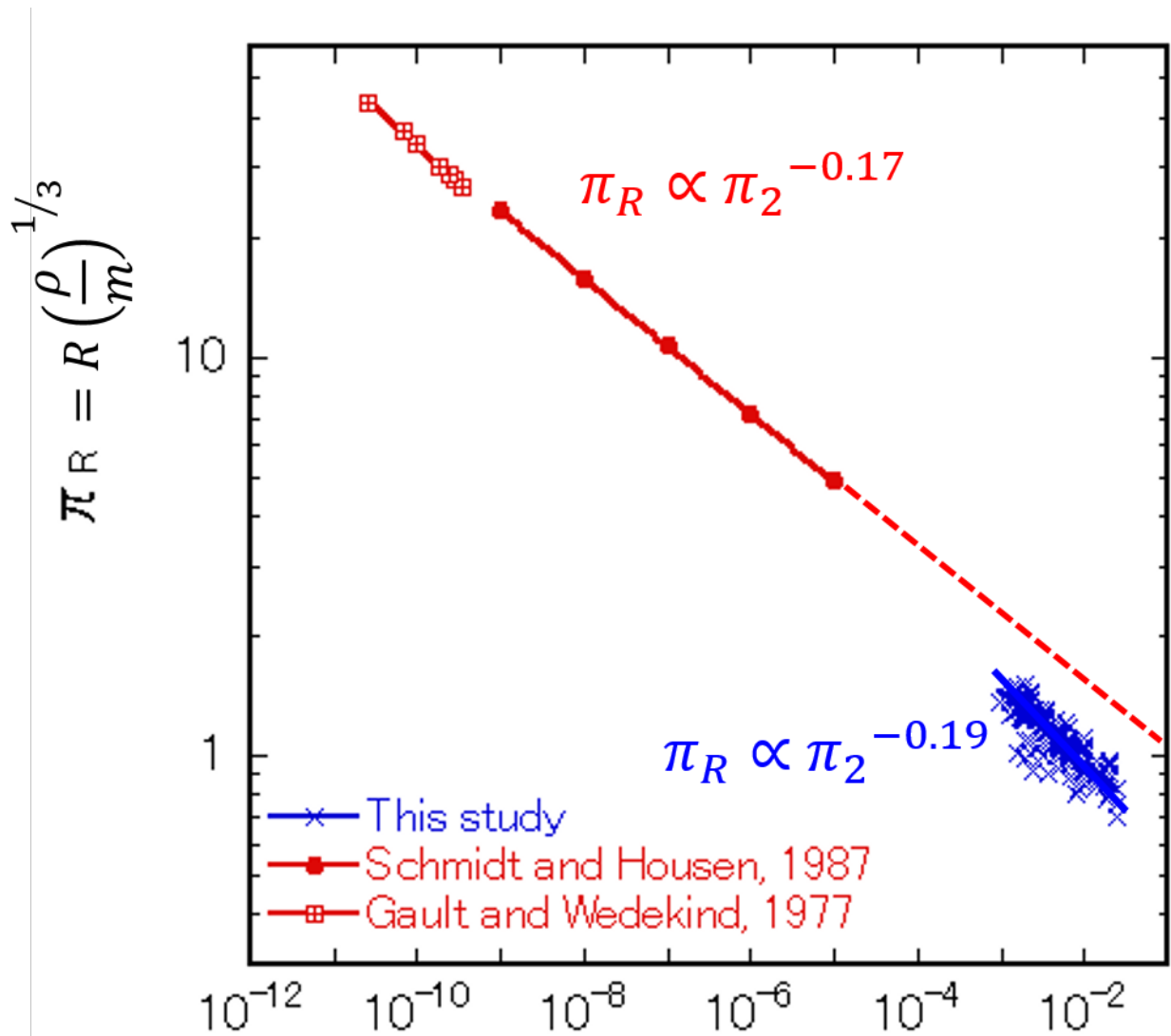
We developed a drop mechanism which can simulate gravities smaller than 1 G. A target container was suspended by springs of constant force, or fallen freely to archive simulated gravity range between 0.01 and 1 G. We used silica sand of average diameter 140  $\mu\text{m}$  as the target material. Stainless steel sphere of 8 mm diameter was impacted onto the target and the impact velocity was between 1 and 5  $\text{ms}^{-1}$ . As a result, the crater diameter was proportional to  $-0.19 \pm 0.01$  power of the gravitational acceleration. This value is roughly in agreement with previous studies at hypervelocity (Kiuchi and Nakamura, 2015 JPGU meeting).

However, the crater diameter obtained by our experiments is not on the line expected from the scaling law (Holsapple, 1993) as shown in the Figure. This difference is caused by a difference of the power-law exponents of  $\pi_2$ ; the exponent is  $-0.19$  for low-velocity impacts and  $-0.17$  for hyper-velocity impacts. A steeper exponent,  $-0.25$ , was obtained for our new impact experiments with glass bead projectiles conducted in the similar setup. These results suggest that the impact energy is consumed for crater formation more efficiently at low-velocity impacts compared to hypervelocity impacts.

We estimated the crater diameter formed by re-impacts of boulders ejected from primary crater on Itokawa based on results of our experiments. We assumed that these boulders impact onto smooth terrain at escape velocity of Itokawa,  $0.17 \text{ ms}^{-1}$ . By combining with these conditions of Itokawa surface and the scaling law obtained by our low-velocity impact experiments, the crater diameter formed by the impact of a boulder of diameter 2 m would be 7 -8 m. Note that the impact velocity assumed was the maximum value and the effect of porosity difference between the laboratory and Itokawa surface was not considered here, however, the estimated crater diameter was consistent with observational data in which the diameter of dimple associated with a boulder of diameter 2m is about 7 m. This result supports the possible low-velocity boulder-impact origin of dimples. We applied similar estimate to boulders derived from Stickney crater of Phobos. As a result, craters which have about 2 to 3 times diameter of boulders would be formed. However, we have not identified dimples associated with boulders on surface images of Phobos. This may be due to a

difference of the surface structure of Itokawa and Phobos and/or due to a difference of surface evolution processes of two bodies.

Keywords: dimple, Itokawa, impact experiments, Phobos



g: gravitational acceleration

a: impactor radius

v: impact velocity, R: crater radius

$\rho$ : target density, m: impactor mass

$$\pi_2 = \frac{ga}{v^2}$$

Earth-moon images captured by Hayabusa2 visible cameras during Earth swing-by

\*Seiji Sugita<sup>1</sup>, Manabu Yamada<sup>2</sup>, Hiroataka Sawada<sup>3</sup>, Tomokatsu Morota<sup>4</sup>, Rie Honda<sup>5</sup>, Shingo Kameda<sup>6</sup>, Chikatoshi Honda<sup>7</sup>, Hidehiko Suzuki<sup>8</sup>, Toru Kouyama<sup>9</sup>, Kazunori Ogawa<sup>10</sup>, MASATERU ISHIGURO<sup>11</sup>

1.the University of Tokyo, 2.Chiba Institute of Technology, 3.JAXA, 4.Nagoya University, 5.Kochi University, 6.Rikkyo University, 7.Aizu University, 8.Meiji University, 9.AIST, 10.Kobe University, 11.Seoul National University

JAXA's Hayabusa2 completed an Earth swing-by on December 3th of 2015. During this opportunity, we photographed both Earth and Moon with three optical navigation cameras (ONC-T, W1 and W2). Since this was the last opportunity to observe extended light source before reaching the target asteroid Ryugu, the obtained images are extremely important for calibration of our cameras. In this paper, we present the Earth-Moon images and preliminary analysis results.

Phase angle dependency on reflectance spectra and ultraviolet spectroscopy of carbonaceous chondrites.

\*Tomohiro Takamatsu<sup>1</sup>, Shingo Kameda<sup>1</sup>, Seiji Sugita<sup>2</sup>

1.School of Science, Rikkyo university, 2.Department of Earth and Planetary Science, Graduate School of Science, The University of Tokyo

The Hayabusa2 spacecraft was launched in 2014, and is expected to arrive at the asteroid Ryugu, which belongs to the C-type asteroids. One of the objectives of the Hayabusa2 mission is to return primordial samples that do not show advanced thermal metamorphism. Vilas (2008) used reflectance spectroscopy from the ground to determine that Ryugu has absorption of approximately 700 nm, indicating the presence of hydrated minerals. The Hayabusa2 spacecraft performs multi-band spectrum observation using ONC-T, which is a telescopic optical navigation camera with seven band-pass filters, and specifies the spot at which the 700 nm absorption feature exists for landing. Therefore, it is important to confirm the detectability of the absorption of 700 nm from multi-band spectral observation. We performed multi-band spectral imaging of carbonaceous chondrites that indicate the same reflectance spectrum as C-type asteroids by using the ONC-T flight model and detected the 700 nm absorption feature at a phase angle of 30° for light-source-sample-ONC-T (Kameda et al, 2015). On the contrary, the phase angle of sun-Ryugu-Hayabusa2 is expected to vary in the range from 0°-40°, while the Hayabusa2 spacecraft is in the vicinity of Ryugu. Therefore, it is also necessary to confirm the detectability of the 700 nm absorption feature in the phase angle of 0°-40° from multi-band spectral observation.

In this study, we perform reflectance spectroscopy of these carbonaceous chondrites using a camera that imitates ONC-T to detect the 700 nm absorption feature in the phase angle range of 0°-40°.

We construct an experimental system in which the incidence angle is variable in the range of 0°-40° and the emission angle is fixed by using a half mirror and a rotation stage. We measure the reflectance spectra and depth of the 700 nm absorption feature of the carbonaceous chondrites using a camera having the same CCD and bandpass filters with nearly identical center wavelengths as that of ONC-T. In this presentation, we report a result.

Moreover, this paper discusses the progress of an investigation about identification of satellite surface materials by ultraviolet observation for a Mars satellite exploration project planned for launch in 2022.

Keywords: Small Solar System Bodies, Multi-band imaging, carbonaceous chondrite

## Effect of iron sulfide on the space weathering of asteroids

Mizuki Okazaki<sup>1</sup>, \*Sho Sasaki<sup>1</sup>, Takahiro Hiroi<sup>2</sup>, Toru Matsumoto<sup>3</sup>, Akira Tsuchiyama<sup>4</sup>, Akira Miyake<sup>4</sup>, Takafumi Hirata<sup>3,4</sup>

1.Department of Earth and Space Sciences, School of Science, Osaka University, 2.Department of Earth, Environmental, and Planetary Sciences, 3.ISAS/JAXA, 4.Department of Earth and Planetary Science, Kyoto University

The space weathering alters surface optical properties on airless bodies such as asteroids, the Moon and Mercury. As for silicate bodies containing iron silicate, the space weathering (characterized by optical reddening, darkening and attenuation of Fe-related absorption) is caused by nanophase metallic iron (npFe<sup>0</sup>) particles within vapor-deposited amorphous rim by micrometeorite impacts or within amorphous rim by solar wind implantation.

However nanophase iron sulfide (npFeS) was found in Itokawa particle's space weathered rim (Noguchi et al., 2011) and was observed more frequently than npFe<sup>0</sup> in regolith breccia meteorites (Noble et al., 2011). Therefore we performed experiments of pulse laser irradiation to olivine and FeS mixture samples to explain the effect of FeS on space weathering. The samples which 5, 10, 20 weight % FeS mixed to olivine of particle size 45-75 micron was made and irradiated at 10 mJ once or twice. Some of laser irradiated samples were also conducted additional thermal fatigue experiments. After laser irradiation and/or thermal fatigue experiments, reflectance spectra of samples were measured, and some of laser irradiation samples were observed by microscopes; FE-SEM, HRM, TEM and SEM-EDS.

The results show FeS promote vapor deposition type space weathering, especially overall darkening. The spectra of samples including FeS showed more reddening and also overall darkening, and also fine FeS particles are highly effective. Thermal fatigue experiments after laser irradiation show that darkening was back to standard but reddening remained. This results show that spectral change especially darkening is not stable against heating simulating asteroidal surface. Our HRM, TEM and SEM-EDS observation suggest npFeS particles exist but have not been exactly identified in this study.

Therefore, addition of FeS particles promote reddening by formatting npFe<sup>0</sup> on the surface of olivine particles. The cause of darkening is not micro-scale particles but macro-scale sulfur deposition by HRM, TEM and SEM-EDS observation. Thermal fatigue experiments in this study show sulfur can easily vaporize from surface, which suggests sulfur on asteroids is less than in meteorites.

Keywords: Space weathering, asteroids, sulfur, reflectance spectrum

## High velocity impact experiments for frozen sands related to crater scaling laws in strength regime

Shota Takano<sup>1</sup>, \*Masahiko Arakawa<sup>1</sup>, Minami Yasui<sup>1</sup>, Kazuma Matsue<sup>1</sup>, Sunao Hasegawa<sup>2</sup>

1.Graduate School of Science, Kobe University, 2.Japan Aerospace Exploration Agency

Solid bodies in the outer solar system are mostly covered with icy crust, and it is composed of ice-rock granular mixture. There are a lot of impact craters on these surfaces, and crater scaling laws are necessary to derive information of impacted bodies from the observed craters and to estimate the regolith thickness deposited on the surface from the ejected material. Especially, on middle and small icy bodies, the crater formation process could be controlled by the material strength of the icy crust, so that the crater scaling laws applicable to the strength regime is necessary to study the crater observed on these small and middle size icy bodies. However, the crater scaling law in the strength regime has not been confirmed by the experiments using the material continuously changing the strength; especially, the ejecta velocity distribution in the strength regime has not been studied yet so far. Therefore, we conducted the impact cratering experiments on the icy material with the various strength to elucidate the material strength dependence on the ejecta velocity distribution and the crater size.

We used frozen quartz sand targets with the water content from 2.5 to 20 wt.%, and they were made at -20 degrees using quartz grain with the size of 100μm. This frozen sample was tested to obtain the tensile strength ( $Y$ ) changing with the water contents ( $C$ ), and the empirical equation was derived as follows,  $Y(\text{MPa})=0.145C$  (wt.%). The impact experiments were conducted at 2, 4 and 6km/s using an aluminum projectile with the diameter of 2mm, and the frozen target was impacted by the projectile on the surface normal to the impact direction.

As a result, the crater formed on the frozen sand with various strength was found to change with the mechanical strength and the crater size increased with the decrease of the strength. The pi-scaling theory for the crater size was applied to these results and the following equation was obtained:  $\pi_R=1.0\pi_Y^{-0.3}$ , where  $\pi_R=R(\rho/m)^{1/3}$ ,  $\pi_Y=Y/\rho v_i^2$ ,  $R$ : crater radius,  $\rho$ : target bulk density,  $m$ : projectile mass, and  $v_i$ : impact velocity. We also measured the ejecta velocity distribution, which was the relationship between the initial ejection position and the ejection angle or the ejection velocity. Then, the ejection angle was found to increase with the distance from the impact point and to become very steep until vertical near the crater rim, and this feature of the ejection angle changing with the distance could cause the unique ejecta curtain called a pillar, which was ejecta curtain extending normal to the target surface. The pillar-like ejecta curtain could be a unique one formed in the strength regime, and it might be originated from the restricted ejecta flow field inside the crater.

Keywords: solar system small bodies, high velocity impact, crater scaling law

## The survey of physical properties of planetary subsurface using penetrator

\*Masashi Okazaki<sup>1</sup>, Masahiko Arakawa<sup>1</sup>, Minami Yasui<sup>1</sup>, Kazuma Matsue<sup>1</sup>, Shota Takano<sup>1</sup>

1. Graduate School of Science, Kobe University

Physical properties of planetary surface such as porosity, grain size etc. are important features to control the thermal and mechanical properties of airless planetary surfaces, then the surfaces such as asteroids and the Moon have been observed by various remote sensing methods. However, the information obtained by the remote sensing is very limited on the mechanical properties of the subsurface layer. While the subsurface mechanical properties are important to elucidate the evolution of the surface geology induced by impacts and tectonics. Then, the exploration method has been studied for the subsurface investigation. A penetrometry is one of the candidates to investigate the subsurface mechanical properties in planetary explorations, and it has been already used for the Cassini-Huygens mission and was planned for Luna-A mission.

In this study, we studied the scientific aspect of the penetrometry, especially for the instrument called as a penetrator. The penetrator usually contains some instruments and can penetrate into planetary subsurface, then it can measure subsurface physical properties during the penetration. Particularly, we focused on the instrument of the accelerometer equipped on the penetrator, which can measure acceleration the resistance force induced from the subsurface materials. The resistance force acquired by the accelerometer on the penetrator would have information of the mechanical properties of the subsurface material. Then, in order to derive the information of the subsurface features from the resistance force, we should know the relationship between the resistance force and the physical properties of the granular layer simulating the subsurface regolith layer.

Therefore, we carried out penetration experiments on various regolith simulant in order to clarify the relationship between the resistance force and the physical properties of the regolith simulant. The resistance force was analyzed to construct the constitutive equation charactering the regolith simulant, and this equation could be useful to analyze the observation in the future mission and to study the evolution of the surface geology.

We used a cylindrical stainless penetrator with the diameter of 2.6cm and the height of 4.35cm. The accelerometer was mounted on the back side of the penetrator, and the penetrator was dropped at various heights to change the penetration velocity and free-fell on the target. We prepared the target by using spherical glass beads (0.5 $\mu$ m, 100 $\mu$ m, 200 $\mu$ m, 500 $\mu$ m, 1mm, 1cm), red clay (2-4mm), quartz sand (100 $\mu$ m, 500 $\mu$ m), and perlite (2-3mm). They were poured into an acrylic cubic case (15cm in each side). The penetrator was dropped through the acrylic cylinder with the inner diameter of 3 cm to control the position of the penetrator and to confirm the impact normal to the target surfaces.

In our experiment, the acquired wave forms showing the resistance forces were evaluated according to the following features: the maximum acceleration value, the acceleration value just before the penetration stop, the duration of the acquired wave. As a result, we found the relationship between the resistance force and the physical properties (porosity, granular size) and constructed the constitution equation for each regolith simulant, and then each equation could be used for the clue to identify the surface materials comparing with the observational data from the penetrator.

Keywords: penetrator, physical property, subsurface



## 54Cr Isotopic Anomalies in Asteroids Caused by Injection and Diffusion in Solar Nebula

\*Taishi Nakamoto<sup>1</sup>, Akira Takeishi<sup>1</sup>

1.Tokyo Institute of Technology

Temporal change of <sup>54</sup>Cr isotopic ratio in meteorites:

Chromium has four stable isotopes: their mass numbers are 50, 52, 53, and 54. The ratio of <sup>54</sup>Cr to the major isotope <sup>52</sup>Cr in various meteorites including chondrites, differentiated meteorites, and iron meteorites shows variations (anomalies). Sugiura and Fujiya (2014) estimated formation ages of each meteorite parent body and found that ages of meteorite parent bodies and the degree of <sup>54</sup>Cr isotopic anomalies in the meteorites are in a good correlation. They thought that this relation is caused by an increase of <sup>54</sup>Cr-rich particles contained in meteorites. Based on this interpretation, they carried out numerical simulations, in which small <sup>54</sup>Cr-rich dust particles are injected into the solar nebula at a certain time and diffuse in the nebula, and showed that the correlation can be reproduced by the small grain injection model.

Injection Model Revisited:

Although the Sugiura and Fujiya model is interesting and attractive, we think some points should be reconsidered. First, they assumed that small dust particles from a supernova arrive only at a narrow ring area on the disk at a certain distance from the central star. However, the injection to such a narrow ring seems unrealistic. Secondly, they supposed that the solar nebula is static. The solar nebula evolves in the time scale not much different from the time scale of parent body formation. Thus, we examine the concentration of <sup>54</sup>Cr-rich dust particles in the solar nebula as a function of time with a uniform injection model. The solar nebula dynamical evolution is also taken into consideration.

Results:

We obtained results that the concentration of <sup>54</sup>Cr-rich grains in the meteorite parent body formation region increases as the time. The surface density of the solar nebula decreases with radial distance, and we suppose that the material is injected uniformly, then after the injection, the concentration of <sup>54</sup>Cr-rich small grains per unit disk area becomes an increasing function of the radial distance. Since the meteorite parent body formation region is rather close to the Sun, e.g., 2 - 4 AU, the concentration in that region is initially low. On the other hand, diffusive motion of small grains in the solar nebula is caused by turbulence, and the mass flux due to the diffusion is in proportion to the gradient of the concentration. So, the distribution of concentration approaches a flat one with time. Thus, the concentration in the meteorite parent body formation region increases with time.

According to our numerical simulations, the quantitative relation between the <sup>54</sup>Cr anomalies and the parent body ages obtained by Sugiura and Fujiya (2014) can be reproduced when the turbulent diffusivity parameter  $a$ , which is a model parameter representing the strength of turbulence in the disk, is of the order of  $10^{-3}$  -  $10^{-2}$ .

Keywords: Isotopic Anomaly, Solar Nebula, 54Cr, Meteorite Parent Body Formation, Injection

#### 4-D calculation of prediction of Perseid

\*Isao Sato<sup>1</sup>, Yushi Imamura<sup>1</sup>, Shinsuke Abe<sup>1</sup>

##### 1.Nihon University

Dust trail theory at present is under the hypothesis that meteoroids have been ejected at the perihelion of the orbit of the parent body of the meteors. However, the meteoroids colliding to the earth have been ejected not at the perihelion but some point on the orbit of the parent body. We reveal that when and where the meteoroids have been ejected on the orbit of the parent body with 3-D velocity vector.

Keywords: meteor, 4-D calculation, perseid

## Possible duplicity of some asteroids discovered in Japan

\*Isao Sato<sup>1</sup>, hamanowa Hiromi, Tomioka Hiroyuki, Uehara Sadaharu, Tsuchikawa Akira

1.Nihon University

We present the possible duplicities of the asteroids (279)Thule, (324)Bamberga, (624)Hektor, (657)Gunlod, and (3220)Murayama which were discovered in Japan.

Keywords: asteroid , satellite

What can be obtained in Mult Impact Hypothesis by Abduction? Approaching the mystery of Origin of "Solar system and Asteroid belt"!

\*Akira Taneko<sup>1</sup>

1.SEED SCIENCE Lab.

The origin of the moon and asteroids, remains unresolved.

There is a distance from the earth, a past of biological birth before, but further experiments impossible.

But can be elucidated in meteorite research, is a rare material available, thermal history by burning at the time of fall is it difficult to origin analysis.

It can not be explained that there is a differentiated meteorites (Stony, iron, stone iron meteorite)

and undifferentiated meteorite.

What can be obtained in Mult Impact Hypothesis by Abduction?

Approaching the mystery of Origin of "Solar system and Asteroid belt"!

Efficacy of abduction is determined all in the selection of "physically meaningful hypothesis".

"That multiple conclusions can be explained systematically without contradiction to each other the current situation" is the proof.

The "Multi-Impact Hypothesis," to give the hypothesis with the following "Linking the moon and the earth of the Missing Link," a unified reasoning of (A) and (B).

(A) Differentiated protoplanetary CERRA of Mars size formed in the asteroid belt position of the solar system, by the perturbation of the most recent of Jupiter (giant mass), orbit is flattened to Jupiter near point side.

(B) Immediately before the CERRA to Jupiter collision, ruptured at a tension of Jupiter and the sun, the mantle piece collide intersects the Earth orbit. by Abduction

(1) Moon of origin: collision mantle piece to Earth (12.4km / s, 36.5 degrees), and formed in the orbit radius  $60 \cdot R_e$  position

\* (2) Pacific Rim arc-shaped archipelago marginal origin: In the Pacific Ocean position collision at the time of moon formation, Depression marginal sea forming in all directions

\* (3) By a large amount of mantle deficient moon formation collision, Van Allen belt of Brazil of core eccentricity (about 10%) was reduced.

\* (4) CERRA it takes about 5-6 million years until the track flat torn in Jupiter perturbation, had already differentiated cooling.

\* (5) Multiple of mantle piece collide to Earth by peeling off the mantle, 70% of the sea surface of the earth -5km was formed by isostasy.

\* (6) Origin of plate tectonics PT, minimization of the eccentric and the moment of inertia caused by the collision as the driving force.

\* (7) Origin of plate boundary, Crust peeling due to the mantle piece collision and crack formation

\* (8) Origin of arc-shaped archipelago and Marginal basin plate: Mantle deficit by collision and plate concave formed by isostasy

\* (9) The origin of the start of subduction convex plate: When the concave plate and the convex plate each other press by the driving force, cause the convex crawl under concave.

(10) Fragments at break of CERRA is the origin of the asteroid belt. Understood in the distribution of long radius (kinetic energy)

(11) The meteorite, but differentiated stony, stony-iron and iron meteorites are mixed, it can be understood with the fragments of CERRA.

(12) There are several fragments of CERRA, large species extinction repeated happened with sequentially collision.

(13) Core and part of the mantle of CERRA, the mass is large energy such as distribution, It became a low orbital energy Mercury with law of equipartition of energy.

(14) The fragments of CERRA that has collided to Jupiter, was the origin of the Great Red Spot.

cf. Shoemaker Levy No. 9 comet collide with Jupiter in July 1997, collision marks remained about half a year as small red spots.

If large Serra of debris from the comet, it is possible to maintain the Great Red Spot without disappear from the hundreds of millions of years ago. Is this in the finished demonstration experiment?

To estimate the origin of the asteroid belt, what to elucidation of purposes in the sample return plan is made clear.

Keywords: the mystery of Origin of " Asteroid belt", Abduction, Multi-Impact Hypothesis, The origin of Asteroid, Origin of differentiated Meteorites, Undifferentiated Meteorite, Chondrite

